**AD-A281 438**

OFFICE OF NAVAL RESEARCH

CHIRAL RECOGNITION IN MOLECULAR AND MACROMOLECULAR PAIRS OF (S)- AND (R)-1-CYANO-2-METHYLPROPYL 4'-{[4-(8-VINYLOXYOCTYLOXY)BENZOYL]OXY}BIPHENYL-4-CARBOXYLATE ENANTIOMERS

by

V. Percec and Q. Zheng

Published

JUL 1 1 1994

in the

Department of Macromolecular Science
Case Western Reserve University
Cleveland, OH 44106-7202

DTIC QUALITY INSPECTED 2

June 30, 1994

**94-20926**

94 7 8 034

# REPORT DOCUMENTATION PAGE

Public reporting burden for this collection of information is estimated to average 1 hour per response, including the time for reviewing instructions, searching existing data sources, gathering and maintaining the data needed, and completing and reviewing the collection of information. Send comments regarding this burden estimate or any other aspect of this collection of information, including suggestions for reducing this burden, to Washington Headquarters Services, Directorate for information Operations and Reports, 1215 Jefferson Davis Highway, Suite 1204, Arlington, VA 22202-4302, and to the Office of Management and Budget, Paperwork Reduction Project (0704-0188), Washington, DC 20503.
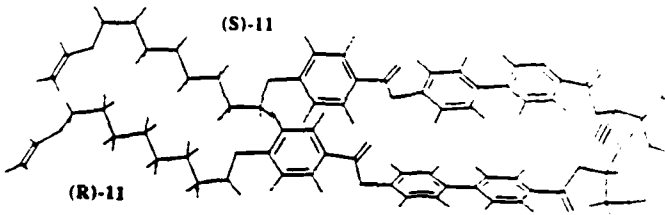
| 1. AGENCY USE ONLY (Leave blank) | 2. REPORT DATE | 3. REPORT TYPE AND DATES COVERED |
|---|---|---|
| | June 30, 1994 | Abstract Report #10 |

| 4. TITLE AND SUBTITLE | 5. FUNDING NUMBERS |
|---|---|
| Chiral Recognition in Molecular and Macromolecular Pairs of (S)- and (R)-1-Cyano-2-Methylpropyl 4'-(4-(8-Vinyloxyoctyloxy)benzoyl)oxy)biphenyl ... | N00014-89-J-1828 |

**6. AUTHOR(S)**

V. Percec and Q. Zheng

| 7. PERFORMING ORGANIZATION NAME(S) AND ADDRESS(ES) | 8. PERFORMING ORGANIZATION REPORT NUMBER |
|---|---|
| Department of Macromolecular Science<br>Case Western Reserve University<br>Cleveland, OH 44106-7202 | N00014-89-J-1828 |

| 9. SPONSORING/MONITORING AGENCY NAME(S) AND ADDRESS(ES) | 10. SPONSORING/MONITORING AGENCY REPORT NUMBER |
|---|---|
| Department of Navy<br>Office of Naval Research<br>800 North Quincy Street<br>Arlington, VA 22217-5000 | Abstract Report #10 |

**11. SUPPLEMENTARY NOTES**

Journal of Chemical Society, Perkin Transactions 1, submitted

| 12a. DISTRIBUTION/AVAILABILITY STATEMENT | 12b. DISTRIBUTION CODE |
|---|---|
| | |

**13. ABSTRACT (Maximum 200 words)**

(S)- and (R)-1-cyano-2-methylpropyl 4'-{[4-(8-vinyloxyoctyloxy)benzoyl]oxy}biphenyl-4-carboxylate [(S)-11 and (R)-11, both > 99% ee] enantiomers and their corresponding homopolymers {poly[(S)-11] and poly[(R)-11]} with well defined molecular weight and narrow molecular weight distribution were synthesized and characterized. The mesomorphic behaviors of (S)-11 and poly[(S)-11] are identical to those of (R)-11 and poly[(R)-11], respectively. Both monomers (S)-11 and (R)-11 exhibit enantiotropic $S_A$, $S_C^*$ and $S_X$ (unidentified smectic) phases. The corresponding homopolymers exhibit $S_A$ and $S_C^*$ phases. The homopolymers with DP < 6 show also a crystalline phase, while those with DP > 10 exhibit a second $S_X$ phase.

Chiral molecular recognition was observed in the $S_A$ and $S_X$ phases of monomers but not in the $S_A$ phase of polymers. In addition, a very unusual chiral molecular recognition effect was detected in the $S_C^*$ phase of monomers below their crystallization temperature and in the $S_C^*$ phase of polymers below their glass transition temperature. In the $S_C^*$ phase of monomers above the melting temperature and of polymers above the glass transition temperature the two enantiomers exhibit nonideal solution behavior. Nonideal solution behavior was also observed in the $S_A$ phase of monomer-polymer and polymer-polymer mixtures.

| 14. SUBJECT TERMS | | 15. NUMBER OF PAGES |
|---|---|---|
| | | |
| | | 16. PRICE CODE |

| 17. SECURITY CLASSIFICATION OF REPORT | 18. SECURITY CLASSIFICATION OF THIS PAGE | 19. SECURITY CLASSIFICATION OF ABSTRACT | 20. LIMITATION OF ABSTRACT |
|---|---|---|---|
| | unclassified | unclassified | UL |

Standard Form 298 (Rev. 2-89)

# Graphical Abstracts for Perkin Trans. 1

## Example

| TITLE | GRAPHICAL ABSTRACT |
|---|---|
| AUTHORS' NAMES | |

## Template

| | |
|---|---|
| Chiral recognition in molecular and macromolecular pairs of (S)- and (R)-1-cyano-2-methylpropyl 4'-{[4-(8-vinyloxyoctyloxy)benzoyl]oxy} biphenyl-4-carboxylate enantiomers<br><br>Virgil Percec and Qiang Zheng | (S)-11<br><br>(R)-11<br>Chiral molecular recognition was observed in the $S_A$. $S_C^*$ and $S_X$ phases of mixtures of (S)-11 with (R)-11 and in the $S_C^*$ phase of the corresponding polymers |

Using the template given above please provide a graphical abstract of the paper and return it to the Editorial Office as soon as possible.

# Chiral Recognition in Molecular and Macromolecular Pairs of (S)- and (R)-1-Cyano-2-Methylpropyl 4'-{[4-(8-Vinyloxyoctyloxy)benzoyl]oxy}biphenyl-4-Carboxylate Enantiomers

Virgil Percec* and Qiang Zheng

Department of Macromolecular Science
Case Western Reserve University
Cleveland, OH 44106

* To whom all correspoundence should be addressed

# ABSTRACT

(S)- and (R)-1-cyano-2-methylpropyl 4'-{[4-(8-vinyloxyoctyloxy)benzoyl]oxy}biphenyl-4-carboxylate [(S)-11 and (R)-11, both > 99% ee] enantiomers and their corresponding homopolymers {poly[(S)-11] and poly[(R)-11]} with well defined molecular weight and narrow molecular weight distribution were synthesized and characterized. The mesomorphic behaviors of (S)-11 and poly[(S)-11] are identical to those of (R)-11 and poly[(R)-11], respectively. Both monomers (S)-11 and (R)-11 exhibit enantiotropic $S_A$, $S_C^*$ and $S_X$ (unidentified smectic) phases. The corresponding homopolymers exhibit $S_A$ and $S_C^*$ phases. The homopolymers with DP < 6 show also a crystalline phase, while those with DP > 10 exhibit a second $S_X$ phase. Phase diagrams were investigated for four different pairs of enantiomers: (S)-11/(R)-11, (S)-11/poly[(R)-11] and poly[(S)-11]/poly[(R)-11] with similar and dissimilar molecular weight. In all cases the structural units derived from the enantiomeric components are miscible and therefore isomorphic in the $S_A$ and $S_C^*$ phases over the entire range of enantiomeric composition.

Chiral molecular recognition was observed in the $S_A$ and $S_X$ phases of monomers but not in the $S_A$ phase of polymers. In addition, a very unusual chiral molecular recognition effect was detected in the $S_C^*$ phase of monomers below their crystallization temperature and in the $S_C^*$ phase of polymers below their glass transition temperature. In the $S_C^*$ phase of monomers above the melting temperature and of polymers above the glass transition temperature the two enantiomers exhibit nonideal solution behavior. Nonideal solution behavior was also observed in the $S_A$ phase of monomer-polymer and polymer-polymer mixtures.

# INTRODUCTION

In the field of liquid crystals chiral molecular recognition was observed in various layered phases of enantiomeric pairs of low molar mass liquid crystals,[1-4] although very little understanding of the influence of structural parameters on its manifestation is available. Molecular recognition in enantiomeric and diastereomeric pairs of macromolecular liquid crystals has not been studied, mainly because of the lack of the techniques available to synthesize enantiomeric and

diastereomeric pairs of liquid crystalline polymers with well controlled molecular weight and narrow molecular weight distribution.

Recently we initiated a systematic series of investigations on the chiral molecular recognition by studying the relationship between molecular, macromolecular and supramolecular structures and the extent of manifestation of heterochiral recognition.[5] The methodology used in our research involves the synthesis of enantiomeric and diastereomeric mesogenic vinyl ethers and of the corresponding homopolymers and copolymers by living cationic polymerization and copolymerization reactions. Living cationic polymerization provides homogeneous polymers and copolymers with well controlled molecular weight, composition and narrow molecular weight distribution.[6,7] Chiral recognition is detected by studying the phase diagrams of monomers, homopolymers and copolymers as a function of enantiomeric composition. In the first publication of this series,[5a] we have reported the observation of the first example of heterochiral recognition in the $S_A$ phase of molecular pairs of diastereomeric liquid crystals based on (2R, 3S)- and (2S, 3S)-2-fluoro-3-methylpentyl 4'-(11-vinyloxyundecanyloxy)biphenyl-4-carboxylate. However, this chiral recognition effect was not observed in the mixture of the two diastereomeric polymers and in the corresponding copolymers. In subsequent publications from this series,[5b,c] heterochiral recognition was observed first in the $S_A$ phase of molecular pairs of enantiomeric liquid crystals based on (R)- and (S)-2-chloro-4-methylpentyl 4'-(8-vinyloxyoctyloxy)biphenyl-4-carboxylate[5b] and (R)- and (S)-2-fluoro-4-methylpentyl 4'-(8-vinyloxyoctyloxy)biphenyl-4-carboxylate,[5c] and also in the $S_C*$ phase of the last pair of enantiomers. In addition, chiral recognition was observed in the same phases of the corresponding homopolymers. However, the copolymers based on the (R)- and (S)-2-chloro-4-methylpentyl 4'-(8-vinyloxyoctyloxy)biphenyl-4-carboxylate enantiomers do not exhibit heterochiral recognition in any of their phases, while the copolymers based on (R)- and (S)-2-fluoro-4-methylpentyl 4'-(8-vinyloxyoctyloxy)biphenyl-4-carboxylate enantiomers display chiral recognition in both their $S_C*$ and $S_X$ phases. The recognition effect observed in the $S_C*$ phase of these copolymers is larger than that observed in their corresponding homopolymer mixtures. The enhancement of the recognition effect in the compounds containing fluorine instead

of chlorine in the stereocenter is considered to be due to the higher electronegativity of fluorine. Therefore, investigation of stereocenters with larger dipoles is of great interest for these studies.

This paper reports the synthesis and living cationic polymerization of a pair of enantiomeric monomers containing a -CN group in their stereocenter i.e., (S)- and (R)-1-cyano-2-methylpropyl 4'-{[4-(8-vinyloxyoctyloxy)benzoyl]oxy}biphenyl-4-carboxylate [(S)-11 and (R)-11]. Heterochiral recognition between the two enantiomers was investigated by studying the phase diagrams of various binary mixtures of monomers and polymers as a function of enantiomeric composition.

## EXPERIMENTAL

### Materials

L-Valine [(S)-2-amino-3-methylbutanoic acid, 99%, Aldrich], methyl chloroformate (99%, Aldrich), tetrabutylammonium hydrogen sulfate (TBAH, 97%, Aldrich), 1,3-dicyclohexylcarbodiimide (DCC, 99%, Aldrich), triphenyl phosphine (PPh3, 99%, Aldrich), ethyl 4-hydroxybenzoate (99%, Aldrich), tris[3-(heptafluoropropyl-hydroxymethylene)-(+)-camphorato], europium(III) derivative [Eu(hfc)3, 98%, Aldrich], benzyl bromide (98%, Fluka) and diethyl azodicarboxylate (DEAD, 90-95%, Fluka), were used as received. Chlorosulfonyl isocyanate (97%, Fluka) was distilled under $N_2$ atmosphere before each use. Dimethyl sulfoxide (DMSO, 99%, Fisher) was heated overnight at 100°C over $CaH_2$, distilled from $CaH_2$ under vacuum, and stored over molecular sieves (4Å). Tetrahydrofuran (THF, 99%, Fisher) was refluxed over $LiAlH_4$ over night and freshly distilled from $LiAlH_4$ before each use.

Methylene chloride (99%, Fisher) used in the cationic polymerization was purified by washing with concentrated sulfuric acid several times until the acid layer remains colorless, then with water, dried over anhydrous $MgSO_4$, refluxed over calcium hydride and freshly distilled under argon before each use. Dimethyl sulfide [$(CH_3)_2S$] (anhydrous, 99+%, packed under nitrogen in Sure/Seal bottle, Aldrich) was distilled over sodium metal under argon.

Trifluoromethanesulfonic acid (CF$_3$SO$_3$H) (98%, Aldrich) was distilled under vacuum. The source of all the other chemicals used was described in the previous publications.[7]

## Techniques

^{1}H-NMR (200 MHz) spectra were recorded on a Varian XL-200 spectrometer, with tetramethylsilane (TMS) as internal standard. Infrared (IR) spectra were recorded on a Perkin-Elmer 1320 infrared spectrophotometer, with samples sandwiched between KBr pellets. The specific rotation of optically active compounds was determined with a Perkin-Elmer 241 polarimeter in solution (the concentration reported is in g/100ml solvent). The enantiomeric excess of monomers was measured by ^{1}H-NMR spectroscopy using Eu(hfc)$_3$ as a shift reagent.

Relative molecular weights of polymers were determined by gel permeation chromatography (GPC) with a Perkin-Elmer Series 10 LC instrument equipped with LC-100 column oven and a Nelson Analytical 900 series integrator data station. A set of two Perkin-Elmer PL gel columns of $5 \times 10^2$ and $10^4$ Å with THF as solvent (1ml/min) and a calibration plot constructed with polystyrene standards were used. High pressure liquid chromatography (HPLC) experiments were performed with the same instrument.

Phase transition temperatures were determined by a Perkin-Elmer DSC-7 differential scanning calorimeter (DSC) equipped with a TAC 7/DX thermal analysis controller. In all cases, heating and cooling rates were 10°C/min unless otherwise indicated. Glass transition temperatures ($T_g$) were read at the middle of the change in the heat capacity. A Carl-Zeiss optical polarized microscope equipped with a Mettler FP 82 hot stage and a Mettler FP 80 central processor was used to observe the thermal transitions and to verify the anisotropic textures.

The dependence of layer spacing of monomers and polymers on temperature was measured by wide angle X-ray scattering (WAXS) experiments (X-ray source: a Rigaku Rotaflex RU-200 D/max rB 12 KW Generator equipped with nickel filtered Cu Kα-radiation and a variable temperature sample holder). The sample was melted into a thin film on an aluminum plate and the

measurement was taken during the heating and/or cooling scan (2.5°C/min) at 2θ ranging from 1.8° to 30°.

## Synthesis of (S)-1-Cyano-2-Methylpropyl 4'-{[4-(8-Vinyloxyoctyloxy)benzoyl]-oxy}biphenyl-4-Carboxylate [(S)-11] and (R)-1-Cyano-2-Methylpropyl 4'-{[4-(8-Vinyloxyoctyloxy)benzoyl]oxy}biphenyl-4-Carboxylate [(R)-11]

The synthetic procedure used for the preparation of monomers (S)-11 and (R)-11 is outlined in Scheme 1. The synthesis of 4'-hydroxybiphenyl-4-carboxylic acid (4) was described elsewhere.[7b]

## (S)-Sodium 2-Hydroxy-3-Methylbutanoate [(S)-2][8]

To a stirred solution of L-valine ($[\alpha]_D^{25}$=+27.5, c=8.0, 6N HCl) (50.0g, 0.43mol) in 650ml of 0.5M $H_2SO_4$ (cooled in an ice bath) was added a solution of $NaNO_2$ (44.3g, 0.64mol) in 120ml of $H_2O$ during 3 h. Evolution of $N_2$ was observed during the addition. After stirring at room temperature for 10 h, the reaction mixture was adjusted to pH=6 by the addition of solid $NaHCO_3$. Then, the solution was adjusted to pH=3 with 40% phosphoric acid. The crude product was extracted by THF (4x150ml). The combined THF extract was washed with brine twice and dried over anhydrous $MgSO_4$. After THF was distilled, a slightly pink oil remained. This was dissolved in 200ml of $CH_3OH$, and the resulting solution was adjusted to pH=7-8 using a concentrated solution of NaOH in $CH_3OH$. The resulting solution was poured into 1200 ml of diethyl ether to produce a white precipitate, which was filtered and dried to give a white powder (39.6g, 66%). $[\alpha]_D^{25}$ = -11.6 (c = 8.03, $H_2O$). IR absorptions (with nüjol on KBr plate) at 1590 and 3300 cm$^{-1}$ indicated the conjugated carbonyl group in -COO$^-$Na$^+$ and -OH group, respectively.

## Synthesis of (S)-Benzyl 2-Hydroxy-3-Methylbutanoate [(S)-3][8]

A mixture of (S)-2 (39.0g, 0.27mol), benzyl bromide (47.9g, 0.27mol) and TBAH (4.8g, 0.01mol) in molecular sieve dried DMF (200ml) was stirred at room temperature for 24 h. DMF was removed by vacuum distillation under 50°C. The resulting suspension was diluted with diethyl ether and filtered. The filtrate was washed with $H_2O$, 5% $NaHCO_3$ and $H_2O$, respectively. After the ether solution was dried over anhydrous $MgSO_4$, the ether was distilled on a rotary evaporator and the resulting liquid was distilled under vacuum to yield a colorless liquid (48.5g, 96.0-99.0°C/0.09mmHg, 83.6%). Purity: > 99% (HPLC). $[\alpha]_D^{25}$=-11.0 (c=0.83, $CHCl_3$). $^1$H-NMR (CDCl$_3$, TMS, δ, ppm): 7.37 (s, 5ArH, -C$_6$H$_5$), 5.22 (s, 2H, -CH$_2$Ph), 4.09 (broad s, 1H, -OH), 2.76(d, J=6.5Hz, 1H, -CH(OH)-), 2.09 (m, 1H, -CH(CH$_3$)$_2$), 1.01-0.84 (2d, J=7.0Hz, 6H, -CH(CH$_3$)$_2$).

## 4'-(Methyloxycarbonyloxy)biphenyl-4-Carboxylic Acid (5)[9]

To a solution of NaOH (14.9g, 0.37mol) in 360ml of $H_2O$ maintained at -10°C, 4 (27.5g, 0.13mol) was added with vigorous stirring. Methyl chloroformate (19.8g, 0.21mol) was added dropwise to the resulting suspension during 1 h. The reaction mixture was stirred at -5°C for 4 h and then was brought to pH=5 by the addition of 20% HCl solution. The resulting white precipitate was filtered off, washed with a large amount of $H_2O$ and dried without further purification to yield 33.5g (95%) of white crystals. mp: 262.2-265.0°C. $^1$H-NMR [(CD$_3$)$_2$CO/DMSO=1/1, TMS, δ, ppm]: 8.09 (d, J=8.0Hz, 2ArH, o to -COOH), 7.60 (d, J=8.6Hz, 4ArH, m to -COOH and m to -OCOO-), 7.33 (d, J=8.7Hz, 2ArH, o to -OCOO-), 3.89 (s, 3H, CH$_3$O-).

## (S)-1-Benzyloxycarbonyl-2-Methylpropyl 4'-(Methyloxycarbonyloxy)biphenyl-4-Carboxylate [(S)-6]

To a suspension containing 5 (9.0g, 33.1mmol), (S)-3 (6.9g, 33.1mmol) and anhydrous 4-dimethylaminopyridinium p-toluene sulfonate (DPTS)[10] (1.9g, 6.5mmol) in a mixture of 80ml

of dry $CH_2Cl_2$ and 50ml dry DMF cooled in ice bath, was added a solution of DCC (7.2g, 33.4mmol) in 20ml of dry $CH_2Cl_2$ during 15 min. The suspension turned to a clear solution during the addition and a precipitate formed in about 30 min. After the reaction mixture was stirred at room temperature for 8 h, the precipitate was filtered and the filtrate was diluted with 100ml of diethyl ether, washed with $H_2O$ and dried over anhydrous $MgSO_4$. The crude product was purified by column chromatography (neutral alumina, diethyl ether/hexane=1/1 as eluent) to yield a colorless viscous liquid (15.2g, 99%). Purity: > 99% (HPLC). $[\alpha]_D^{25}$=+3.72 (c=1.00, CHCl$_3$). $^1$H-NMR (CDCl$_3$, TMS, δ, ppm): 8.15 (d, J=8.5Hz, 2ArH, o to -COO-), 7.65 (d, J=7.9Hz, 2ArH, m to -COO-), 7.63 (d, J=8.8Hz, 2ArH, m to -OCOO-), 7.34 (s, 5ArH, -CH$_2$-C$_6$H$_5$), 7.30 (d, J=10.3Hz, 2ArH, o to -OCOO-), 5.22 (d, J=2.3Hz, 2H, -CH$_2$Ph), 5.15 (d, J=6.2Hz, 1H, -COOCH(COOCH$_2$Ph)-), 3.93 (s, 3H, CH$_3$O-), 2.39 (m, 1H, -CH(CH$_3$)$_2$), 1.10-1.06 (2d, J=7.0Hz, 6H, -CH(CH$_3$)$_2$).


**(R)-1-Benzyloxycarbonyl-2-Methylpropyl 4'-(Methyloxycarbonyloxy)biphenyl-4-Carboxylate [(R)-6][1]**

A suspension of **5** (9.0g, 33.1mmol), **(S)-3** (6.9g, 33.1mmol) and PPh$_3$ (8.77g, 33.1mmol) in 100ml of dry THF was cooled in an ice bath. DEAD (6.4g, 33.1mmol) was added dropwise during 20 min. and the suspension turned into a clear light yellow solution during the addition. The solution was stirred at room temperature for 12 h and the solvent was distilled in a rotary evaporator to give a light yellow thick suspension, which was subjected to column chromatography (neutral alumina, diethyl ether/hexane=1/1 as eluent) to yield a colorless viscous liquid (8.0g, 52%). Purity: > 99% (HPLC). $[\alpha]_D^{25}$=-3.70 (c=0.99, CHCl$_3$). $^1$H-NMR (CDCl$_3$, TMS, δ, ppm): 8.15 (d, J=8.6Hz, 2ArH, o to -COO-), 7.65 (d, J=8.2Hz, 2ArH, m to -COO-), 7.63 (d, J=8.5Hz, 2ArH, m to -OCOO-), 7.34 (s, 5ArH, -CH$_2$-C$_6$H$_5$), 7.30 (d, J=10.6Hz, 2ArH, o to -OCOO-), 5.22 (d, J=3.0Hz, 2H, -CH$_2$Ph), 5.16 (d, J=6.1Hz, 1H, -COOCH(COOCH$_2$Ph)-), 3.93 (s, 3H, CH$_3$O-), 2.40 (m, 1H, -CH(CH$_3$)$_2$), 1.10-1.07 (2d, J=6.8Hz, 6H, -CH(CH$_3$)$_2$).

(S)-1-Carboxy-2-Methylpropyl 4'-(Methyloxycarbonyloxy)biphenyl-4-Carboxylate [(S)-7]

(S)-6 (14.0g, 31.8mmol) was dissolved in 150ml of ethyl acetate containing 5% Pd-on-charcoal (0.7g). The resulting suspension was stirred under $H_2$ atmosphere (50 psi) at room temperature for 8 h to complete the hydrogenolysis of the benzyl ester (monitored by using TLC). The catalyst was filtered off and the filtrate was evaporated to dryness to give a white solid (10.6g, 95%. Purity: > 99%. mp: 118.5-120.0°C. $[\alpha]_D^{25}$=+37.30 (c=1.05, $CHCl_3$). $^1$H-NMR (CDCl$_3$, TMS, δ, ppm): 8.16 (d, J=9.4Hz, 2ArH, o to -COO-), 7.67 (d, J=7.7Hz, 2ArH, m to -COO-), 7.65 (d, J=8.3Hz, 2ArH, m to -OCOO-), 7.30 (d, J=8.3Hz, 2ArH, o to -OCOO-), 5.17 (d, J=4.4Hz, 1H, -COOC$\underline{H}$(COOH)-), 3.94 (s, 3H, C$\underline{H}_3$O-), 2.44 (m, 1H, -C$\underline{H}$(CH$_3$)$_2$), 1.18-1.13 (2d, J=8.0Hz, 6H, -CH(C$\underline{H}_3$)$_2$).

(R)-1-Carboxy-2-Methylpropyl 4'-(Methyloxycarbonyloxy)biphenyl-4-Carboxylate [(R)-7]

(R)-7 was prepared from (R)-6 by the same method as (S)-7. Starting from (R)-6 (8.0g, 21.5mmol), a white solid was obtained (5.1g, 80%). Purity: > 99%. mp: 118.8-120.0°C. $[\alpha]_D^{25}$ = -37.34 (c = 1.10, CHCl$_3$). $^1$H-NMR (CDCl$_3$, TMS, δ, ppm): 8.15 (d, J=8.9Hz, 2ArH, o to -COO-), 7.66 (d, J=7.6Hz, 2ArH, m to -COO-), 7.65 (d, J=8.5Hz, 2ArH, m to -OCOO-), 7.28 (d, J=8.5Hz, 2ArH, o to -OCOO-), 5.17 (d, J=4.3Hz, 1H, -COOC$\underline{H}$(COOH)-), 3.94 (s, 3H, C$\underline{H}_3$O-), 2.44 (m, 1H, -C$\underline{H}$(CH$_3$)$_2$), 1.17-1-13 (2d, J=5.8Hz, 6H, -CH(C$\underline{H}_3$)$_2$).

(S)-1-Cyano-2-Methylpropyl 4'-(Methyloxycarbonyloxy)biphenyl-4-Carboxylate [(S)-8][12]

Chlorosulfonyl isocyanate (5.7g, 40.2mmol) was added dropwise at room temperature during 15 min to a solution of (S)-7 (7.5g, 20.1mmol) in 25ml of dry $CH_2Cl_2$. The reaction mixture was refluxed for 1 h and then was distilled under vacuum to remove the solvent and the excess of chlorosulfonyl isocyanate. Dry $CH_2Cl_2$ (10ml) was introduced under a $N_2$ atmosphere

and the resulting light yellow solution was cooled in an ice bath. Dry DMF (20ml) was then added slowly and the solution was stirred at room temperature for 1 h. The reaction mixture was then poured into 100ml of water, and extracted with diethyl ether (4x50ml). The combined ether solution was washed with 5% $NaHCO_3$ and $H_2O$, and dried over anhydrous $MgSO_4$. The ether solution was distilled in a rotary evaporator to give a light yellow oil, which was purified by column chromatography (neutral alumina, diethyl ether/hexane=2/1 as eluent) to yield a white solid (4.4g, 62%). Purity: > 99%, mp: 71.6-72.9°C. $[\alpha]_D^{25}$=-8.16 (c=1.00, $CHCl_3$). $^1$H-NMR (CDCl$_3$, TMS, δ, ppm): 8.14 (d, J=8.2Hz, 2ArH, o to -COO-), 7.67 (2d, J=8.1Hz, 4ArH, m to -COO- and m to -OCOO-), 7.35 (d, J=8.9Hz, 2ArH, o to -OCOO-), 5.48 (d, J=5.9Hz, 1H, -COOCH(CN)-), 3.94 (s, 3H, CH$_3$O-), 2.32 (m, 1H, -CH(CH$_3$)$_2$), 1.21 (t, J=7.4Hz, 6H, -CH(CH$_3$)$_2$).

## (R)-1-Cyano-2-Methylpropyl 4'-(Methyloxycarbonyloxy)biphenyl-4-Carboxylate [(R)-8]

Starting from (R)-7 (3.5g, 9.4mmol) and chlorosulfonyl isocyanate (2.7g, 19.0mmol), (R)-8 (2.1g, 61%) was obtained as a white solid by a similar procedure to that used in the case of (S)-8. Purity: > 99%, mp: 71.6-73.1°C. $[\alpha]_D^{25}$=+8.16 (c=1.02, $CHCl_3$). $^1$H-NMR (CDCl$_3$, TMS, δ, ppm): 8.14 (d, J=8.0Hz, 2ArH, o to -COO-), 7.67 (2d, J=8.3Hz, 4ArH, m to -COO- and m to -OCOO-), 7.35 (d, J=8.6Hz, 2ArH, o to -OCOO-), 5.48 (d, J=6.0Hz, 1H, -COOCH(CN)-), 3.94 (s, 3H, CH$_3$O-), 2.33 (m, 1H, -CH(CH$_3$)$_2$), 1.22 (t, J=7.4Hz, 6H, -CH(CH$_3$)$_2$).

## (S)-1-Cyano-2-Methylpropyl 4'-(Hydroxy)biphenyl-4-Carboxylate [(S)-9][9]

(S)-8 (4.15g, 11.7mmol) was stirred in a mixture of 300ml of ethanol and 150ml of aqueous ammonia (10-35%) at room temperature for 1 h. The reaction mixture was poured into 300ml of water. The crude product was extracted with $CH_2Cl_2$ (4x80ml) and the combined $CH_2Cl_2$ solution was washed with 6M HCl, 5% $NaHCO_3$ and water, respectively. The crude

product was purified by column chromatography (silica gel, hexane/ethyl acetate=6/1 as eluent) to yield a white solid (2.8g, 82%). Purity: > 99%, mp: 103.1-104.5°C $[\alpha]_D^{25}$=-4.40 (c=1.07, CHCl₃). ¹H-NMR (CDCl₃, TMS, δ, ppm): 8.10 (d, J=8.0Hz, 2ArH, o to -COO-), 7.66 (d, J=8.6Hz, 2ArH, m to -COO-), 7.54(d, J=8.5Hz, 2ArH, m to -OH), 6.96 (d, J=9.4Hz, 2ArH, o to -OH), 5.47 (d, J=5.4Hz, 1H, -COOCH(CN)-), 5.37(s, 1H, -OH), 2.34 (m, 1H, -CH(CH₃)₂), 1.21 (t, J=7.3Hz, 6H, -CH(CH₃)₂).

### (R)-1-Cyano-2-Methylpropyl 4'-(Hydroxy)biphenyl-4-Carboxylate [(R)-9]

(R)-9 (1.2g, 72%) was obtained from (R)-8 (2.0g, 5.7mmol) by the same method as (S)-9. Purity: > 99%. mp: 103.0-104.7°C. $[\alpha]_D^{25}$=+4.39 (c=1.01, CHCl₃). ¹H-NMR (CDCl₃, TMS, δ, ppm): 8.10 (d, J=8.0Hz, 2ArH, o to -COO-), 7.66 (d, J=8.5Hz, 2ArH, m to -COO-), 7.54 (d, J=8.7Hz, 2ArH, m to -OH), 6.96 (d, J=8.8Hz, 2ArH, o to -OH), 5.47 (d, J=5.3Hz, 1H, -COOCH(CN)-), 5.37 (s, 1H, -OH), 2.34 (m, 1H, -CH(CH₃)₂), 1.21 (t, J=7.1Hz, 6H, -CH(CH₃)₂).

### 4-(8-Vinyloxyoctyloxy)benzoic Acid (10)

Ethyl 4-hydroxybenzoate (2.24g, 13.3mmol) and NaOH (0.54g, 13.5mmol) were dissolved in 80ml 95% ethanol and heated to reflux for 15 min. 8-Vinyloxyoctylbromide[7c] (3.17g, 13.5mmol) was added and the reaction mixture was refluxed for 14 h and poured into 200ml of water. The crude product was extracted with diethyl ether and purified by column chromatography (silica gel, $CH_2Cl_2/C_6H_{14}$=2/1 as eluent) to give ethyl 4-(8-vinyloxyoctyloxy)benzoate as a colorless liquid (3.1 g, 72%). Purity: > 99%. ¹H-NMR (CDCl₃, TMS, δ, ppm): 8.00 (d, J=8.0Hz, 2ArH, o to -COO-), 6.91 (d, J=8.6Hz, 2ArH, m to -COO-), 6.53-6.42 (q, J=7.0Hz, 1H, CH₂=CH-), 4.35 (q, J=6.1Hz, 2H, -COOCH₂-), 4.17(d, J=3.6Hz, 1H, cis CH₂=CH-), 4.00 (m, 3H, trans CH₂=CH- and -PhOCH₂-), 3.68 (t, J=6.9Hz, 2H, =CHOCH₂), 1.77 (m, 2H, -PhOCH₂CH₂-), 1.67 (m, 2H, =CHOCH₂CH₂-), 1.38 (m, 11H, -O(CH₂)₂(CH₂)₄- and -CH₂CH₃). Ethyl 4-(8-vinyloxyoctyloxy)benzoate (3.1g, 13.3mmol) was

hydrolyzed at 60°C for 1 h in 60ml of 95% ethanol containing KOH (2.7g, 48.4mmol). The resulting solution was cooled and acidified with 1N HCl. The precipitate was filtered, dried in air and recrystallized from 95% ethanol to afford white crystals (2.4g, 85%). $^1$H-NMR (CDCl$_3$, TMS, δ, ppm): 8.06 (d, J=8.1Hz, 2ArH, o to -COOH), 6.94 (d, J=8.6Hz, 2ArH, m to -COOH), 6.53-6.42 (q, J=7.0Hz, 1H, CH2=CH-), 4.17(d, J=4.0Hz, 1H, cis CH2=CH-), 4.03 (m, 3H, trans CH2=CH- and -PhOCH2-), 3.68 (t, J=7.1Hz, 2H, =CHOCH2), 1.79 (m, 2H, -PhOCH2CH2-), 1.66 (m, 2H, =CHOCH2CH2-), 1.37 (m, 8H, -O(CH2)2(CH2)4-).

## (S)-1-Cyano-2-Methylpropyl 4'-{[4-(8-Vinyloxyoctyloxy)benzoyl]oxy}biphenyl-.-Carboxylate [(S)-11]

Into a suspension of (S)-9 (1.0g, 3.4mmol), 10 (1.0g, 3.4mmol) and DPTS (0.2g, 0.7mmol) in 15ml of dry CH2Cl2 was added dropwise a solution of DCC (0.73g, 3.6mmol) in 2ml of CH2Cl2 dropwise at room temperature. The reaction mixture first became a clear solution. Then a precipitate formed. After stirring at room temperature for 8 h, the reaction mixture was diluted with 50ml of diethyl ether and then was filtered. The filtrate was poured into 100 ml of ice water and extracted with diethyl ether (4x50ml). The combined ether solution was washed with water, and dried over anhydrous MgSO4. The crude product was purified by column chromatography (silica gel, CH2Cl2/C6H14=6/1 as eluent) and finally was recrystallized from methanol to yield white crystals (1.4 g, 74%). Purity: > 99%. Enantiomeric excess: > 99% ($^1$H-NMR). Phase transitions: K 106.2°C S$_A$ 120.1°C i (DSC, 10°C/min). $[\alpha]_D^{25}$=-3.07 (c=1.07, CHCl3). $^1$H-NMR (CDCl3, TMS, δ, ppm): 8.16 (2d, J=11.2Hz, 4ArH, o to -COO-), 7.71 (2d, J=7.5Hz, 4ArH, m to -COO-), 7.34(d, J=8.3Hz, 2ArH, m to -OCO-), 7.00 (d, J=8.8Hz, 2ArH, o to -OCH2-), 6.54-6.43 (q, J=7.1Hz, 1H, CH2=CH-), 5.48 (d, J=6.0Hz, 1H, -COOCH(CN), 4.18 (d, J=3.8Hz, 1H, cis CH2=CH-), 4.06 (t, J=6.3Hz, 2H, -PhOCH2-), 3.99 (d, J=6.6Hz, 1H, trans CH2=CH-), 3.69 (t, J=6.5Hz, 2H, =CHOCH2), 2.33 (m, 1H, -CH(CH3)2), 1.83 (m, 2H, -PhOCH2CH2-), 1.68 (m, 2H, =CHOCH2CH2-), 1.39 (m, 8H, -O(CH2)2(CH2)4-), 1.22 (t, J=6.6Hz, 6H, -CH(CH3)2).

(R)-1-Cyano-2-Methylpropyl 4'-{[4-(8-Vinyloxyoctyloxy)benzoyl]oxy}biphenyl-4-Carboxylate [(R)-11]

White crystals of (R)-11 (1.5g, 76%) were obtained by following an identical procedure as in the case of (S)-11. Purity: > 99%. Enantiomeric excess: > 99% ($^1$H-NMR). Phase transitions: K 106.1°C $S_A$ 120.0°C i (DSC, 10°C/min). $[\alpha]_D^{25}$=+3.07 (c=1.07, $CHCl_3$). $^1$H-NMR ($CDCl_3$, TMS, δ, ppm): 8.16 (2d, J=11.2Hz, 4ArH, o to -COO-), 7.70 (2d, J=7.6Hz, 4ArH, m to -COO-), 7.34(d, J=8.3Hz, 2ArH, m to -OCO-), 7.00 (d, J=7.6Hz, 2ArH, o to -OCH$_2$-), 6.54-6.43 (q, J=7.1Hz, 1H, CH$_2$=CH-), 5.48 (d, J=6.0Hz, 1H, -COOCH(CN), 4.18 (d, J=3.8Hz, 1H, cis CH$_2$=CH-), 4.06 (t, J=6.3Hz, 2H, -PhOCH$_2$-), 3.98 (d, J=6.4Hz, 1H, trans CH$_2$=CH-), 3.69 (t, J=6.4Hz, 2H, =CHOCH$_2$), 2.34 (m, 1H, -CH(CH$_3$)$_2$), 1.84 (m, 2H, -PhOCH$_2$CH$_2$-), 1.67 (m, 2H, =CHOCH$_2$CH$_2$-), 1.39 (m, 8H, -O(CH$_2$)$_2$(CH$_2$)$_4$-), 1.22 (t, J=6.7Hz, 6H, -CH(CH$_3$)$_2$).

## Cationic Polymerizations

Polymerizations were carried out in a three-neck round bottom flask equipped with a stopcock and rubber septum under argon atmosphere at 0°C for 1 h. All glassware was dried overnight at 140°C. The monomer was further dried under vacuum overnight in the polymerization flask. After the flask was filled with argon, freshly distilled dry $CH_2Cl_2$ was added through a syringe and the solution was cooled to 0°C. Freshly distilled $(CH_3)_2S$ and $CF_3SO_3H$ were then added consecutively via syringes. The monomer concentration was about 0.2M and the $(CH_3)_2S$ concentration was 10 times larger than that of the $CF_3SO_3H$ used as an initiator. The polymer molecular weight was controlled by the monomer/initiator ($[M]_o/[I]_o$) ratio. After quenching the polymerization with $NH_4OH$ and $CH_3OH$, the reaction mixture was precipitated into methanol. The filtered polymers were purified by precipitation from $CH_2Cl_2$ solution into $CH_3OH$. The resulting polymers were dried in a vacuum oven at room temperature.

# RESULTS AND DISCUSSION

## 1. Synthesis of monomers (S)-11 and (R)-11

The synthesis of monomers (S)-11 and (R)-11 is presented in Scheme 1. L-Valine was reacted with HNO₂ between -5 and 0°C in aqueous solution to give (S)-2-hydroxy-3-methylbutanoic acid with retention of original (S) configuration due to the anchimeric assistance provided by the carboxylate group.[13] A similar mechanism was valid for the replacement of the amino group with chlorine via the diazonium salt intermediate. Complete retention of configuration during this reaction was observed for most of the optically active amino acids.[14,15] The carboxylic acid group of (S)-2-hydroxy-3-methylbutanoic acid was neutralized with NaOH to give (S)-sodium 2-hydroxy-3-methylbutanoate [(S)-2] and then was esterified with benzyl bromide to produce (S)-3. Methyl chloroformate was used to protect the phenol group of 4 to give 5. (S)-6 was prepared by the esterification of (S)-3 with 5 in the presence of DCC and DPTS. This reaction takes place with the retention of configuration of the chiral center.

The esterification of (S)-3 with 5 in the presence of DEAD and PPh₃ yields (R)-6 with the inversion of configuration of the stereocenter of (S)-3. The general mechanism[11] of this reaction is outlined in Scheme 2. In this reaction, DEAD (12) and PPh₃ (13) reacted to generate the quaternary phosphonium salt (14). 14 was protonated by an acid (15), forming a second quaternary phosphonium salt (16). The nucleophilic attack by a chiral alcohol (17) gives an alkoxyphosphonium salt (18), which undergoes $S_N2$ type displacement to afford the product 20 with inversion of configuration.[11,16,17]

The benzyl ester protecting group of (S)-6 and (R)-6 was removed by hydrogenolysis to produce (S)-7 and (R)-7, respectively. Afterwards, the -COOH group of (S)-7 and (R)-7 was converted to -CN by treating the acid with ClSO₂NCO in CH₂Cl₂ and DMF.[12] The deprotection of methyl carbonate of (S)-8 and (R)-8 was carried out with 30% NH₄OH in ethanol[9] to yield (S)-9 and (R)-9, which were reacted with 10 in the presence of DCC and DPTS to produce monomers (S)-11 and (R)-11.

## 2. Optical purities of (S)-11 and (R)-11

The optical purities of monomers **(S)-11** and **(R)-11** were determined by 200 MHz $^1$H-NMR spectroscopy using Eu(hfc)$_3$ as a chiral shift reagent. The $^1$H-NMR spectra of **(S)-11** and **(R)-11** recorded in CDCl$_3$ are identical. Figure 1a presents representative $^1$H-NMR spectra of **(S)-11** without, while Figure 1b with the shift reagent. Figure 2a and b presents the $^1$H-NMR spectra of the monomer mixture (molar ratio of **(S)-11**/**(R)-11**=2/1) without and with the shift reagent, respectively. In Figure 1a the doublet at $\delta$=5.48 (J=6.0) is due to the proton of the cyanohydrin ester [-COOC$\underline{\text{H}}$(CN)-]. When the shift reagent Eu(hfc)$_3$ was added incrementally to the monomer solution, the doublet shifted to a higher field and its coupling constant as indicated in Figure 1b did not change (J=6.0). Although the $^1$H-NMR spectra of **(S)-11** and **(R)-11** monomer mixture (molar ratio of **(S)-11**/**(R)-11**=2/1) (Figure 2a) looks identical to that of **(S)-11**, the addition of the shift reagent clearly separated two doublets. The doublet at $\delta$=6.02 (J=6.0) is due to the cyanohydrin ester hydrogen in **(S)-11** and the other at $\delta$=6.14 (J=6.0) is due to the cyanohydrin ester hydrogen in **(R)-11**. The integration of these two doublets is 2/1, reflecting the initial molar ratio of the two monomers in the mixture. As the amount of the shift reagent increases, the separation of these two doublets become larger and they are shifted to an even higher field. However, the coupling constant of both doublets remains unchanged. This separation behavior by the chiral shift reagent is due to the different interaction between the pure enantiomers with the chiral shift reagent. Both monomers were carefully checked by $^1$H-NMR with the Eu(hfc)$_3$. The optical purities of both monomers [**(S)-11** and **(R)-11**] are higher than 99% ee.

## 3. Polymerization of (S)-11 and (R)-11 and Characterization of Poly[(S)-11] and Poly[(R)-11]

Previous publications from our[6,7,18] and other laboratories[19] have demonstrated that polymerization of functional vinyl ethers initiated by (CF$_3$SO$_3$H/(CH$_3$)$_2$S system exhibits the characteristics of a living polymerization, leading to well defined polymers with controlled molecular weights and narrow polydispersities. Therefore both monomers **(S)-11** and **(R)-11**

were polymerized using $CF_3SO_3H/(CH_3)_2S$ at $0^oC$ in dry $CH_2Cl_2$. The resulting polymers were characterized by GPC, DSC and thermal optical polarized microscopy. Selected polymer samples were also characterized by wide angle X-ray scattering (WAXS) measurements to confirm the nature of the mesophases assigned by optical polarized microscopy. The characterization results are summarized in Tables 1 and 2.

Polymer yields are between 50 and 70%. The low polymer yields are due to a combination of the polymer loss during the purification process and the small scale polymerization experiments (100 mg). Within the experimental error the relative number average molecular weights (Mn) of both poly[(S)-11] and poly[(R)-11] are well controlled by the initial molar ratio of monomer to initiator ($[M]_o/[I]_o$). A characteristic linear dependence of Mn on $[M]_o/[I]_o$ is shown in Figure 3. The polydispersities of all polymers are less than 1.20. All these features support the characteristics of a living polymerization.

The mesomorphic behavior of poly[(S)-11] and poly[(R)-11] was characterized by DSC. The thermal transition temperatures and the nature of various mesophases were confirmed by thermal optical polarized microscopy. The DSC thermograms of the first heating scan ($20^oC$) are presented in Figure 4a and b for poly[(S)-11] and poly[(R)-11], respectively. Thermal decomposition of poly[(S)-11]s and poly[(R)-11]s with DP larger than 6 was observed after the first heating scan when the isotropization temperature exceeded $200^oC$. $^1H$-NMR spectra of the samples collected from the DSC pan indicate that the decomposition of cyanohydrin esters and some kind of transesterification might take place. Figure 4a shows that all poly[(S)-11]s with different degrees of polymerization (DP) exhibit enantiotropic $S_C^*$ and $S_A$ phases. Poly[(S)-11]s with DP ≤ 5.4 also show a crystalline phase below $55^oC$. The disappearance of this crystalline phase in polymers with higher DP is probably due to the decreased chain mobility. Poly[(S)-11]s with DP ≥ 10.1 exhibit an unidentified smectic phase ($S_X$ phase). The nature of the $S_X$ phase is not identified yet at this moment. The DSCs scans of poly[(R)-11]s (Figure 4b) are quite similar to those of poly[(S)-11]s. Their phase behavior can be compared in Figure 5 by superimposing the dependence of their thermal transition temperatures on DP. It is clear that the mesomorphic

behavior of poly[(S)-11]s is identical to that of poly[(R)-11]s. Without polymers containing well controlled molecular weights and narrow polydispersities, no such comparison could be made. Misleading conclusions can be drawn if we do not have the entire dependence of phase transitions on molecular weight.

In order to further confirm the $S_C^*$ and $S_A$ phases of both homopolymers, WAXS experiments were carried out. The results obtained from WAXS are shown in Figure 6a and b, where representative scattering patterns in each of the $S_A$, $S_C^*$ and $S_X$ phases and the dependence of the layer spacing obtained during the heating scan (2.5°C/min) on temperature are presented. In Figure 6a all three scattering patterns show a sharp peak due to the layer structure of the smectic phase. The additional peaks in $S_X$ phase can be related to the additional position order within the smectic layer. As observed from Figure 6b, the layer spacing of both homopolymers increases with increasing the temperature within the range of the $S_C^*$ phase, and then remains constant at $31.5 \pm 0.5$ Å from 150°C on, where the $S_A$ phase is formed. The behavior of the layer spacing as a function of temperature is in good agreement with the phase transition temperatures and the nature of mesophases determined by DSC and optical polarized microscopy. The experimental value ($31.5 \pm 0.5$ Å) of the layer spacing in the $S_A$ phase is consistent with the calculated value (32.6 Å) of the fully extended mesogenic unit. Therefore, these results support the existence of $S_A$ and $S_C^*$ phases in both homopolymers.

## 4. Mesomorphic behavior and heterochiral molecular recognition in mixtures of enantiomeric monomers and polymers

The first order phase transition temperature of a binary mixture of an ideal solution can be predicted by the Schröder-van Laar equation:[20]

$$x_1 = \left[ 1 - \frac{\Delta H_1 T_2 (T - T_1)}{\Delta H_2 T_1 (T - T_2)} \right]^{-1}$$

where, $x_1$ is the mole fraction of compound 1; $T_1$ and $T_2$ are the transition temperatures; $\Delta H_1$ and $\Delta H_2$ are the corresponding enthalpy changes; and T is the transition temperature of the mixture.

Assuming that the transition temperatures of the two components are in the order of $T_1 \leq T_2$, the transition temperatures of the mixtures as a function of composition follow one of the following three ideal cases if an ideal solution is formed. Case 1) when the enthalpy changes $\Delta H_1 \approx \Delta H_2$, the transition temperatures of the mixture should show a linear dependence on composition; Case 2) when $\Delta H_1 < \Delta H_2$, the transition temperatures will exhibit an upward curvature; and Case 3) when $\Delta H_1 > \Delta H_2$, the transition temperatures will show a downward curvature. Chiral recognition leads to a nonideal solution behavior for the case of an ideal mixture. Chiral recognition is present when a positive deviation from the ideal solution behavior dependence predicted by the Schröder-van Laar equation which is due to an interaction between the two enantiomers (heterochiral recognition) is observed. Heterochiral recognition requires first that the two compounds are miscible at the molecular level. On the other hand, a negative deviation from the ideal behavior is an other manifestation of a nonideal solution behavior which is caused by the immiscibility of the two compounds at the molecular level.

In order to study the heterochiral recognition in pairs of enantiomeric monomers and polymers, miscibility studies were carried out by preparing four pairs from the following mixtures: (S)-11/(R)-11, (S)-11/poly[(R)-11] with DP=4.4, poly[(S)-11] with DP=4.6/poly[(R)-11] with DP=4.4 and poly[(S)-11] with DP=4.3/poly[(R)-11] with DP=5.7. These mixtures can be categorized into three groups: a) binary mixtures of monomers; b) binary mixtures of monomer and polymer; and c) binary mixtures of polymers with similar and dissimilar molecular weights. All these mixtures were prepared by dissolving the two components in $CH_2Cl_2$, followed by the evaporation of solvent in the vacuum oven for at least 24 h at room temperature.

## 4a) Mixtures of monomers

The DSC traces of monomer mixtures (S)-11/(R)-11(X/Y) [where X/Y is the molar ratio of (S)-11 to (R)-11] are presented in Figure 7. The phase diagrams of the monomer mixtures are provided in Figure 8. The phase transition temperatures and corresponding enthalpy changes are summarized in Table 3.

Figure 7a, b and d presents the first and second heating, and first cooling scans of (S)-11/(R)-11(X/Y). Subsequent heating and cooling scans are identical to the second heating and first cooling scans, respectively. In order to reveal the phase transition from $S_C^*$ to $S_A$ for (S)-11/(R)-11(X/Y) with X/Y=70/30-30/70, an additional heating scan was performed by cooling the sample only up to 50°C followed by reheating from 50°C. The resulting DSC curves are presented in Figure 7c. This experiment allows the kinetically controlled crystalline phases which cover the $S_C^*$-$S_A$ transition in (S)-11/(R)-11(X/Y) with X/Y = 70/30-30/70 to be suppressed. As observed in Figure 7, the phase behaviors of the two enantiomers (S)-11 and (R)-11 are identical. In the first DSC scan (Figure 7a) the optical pure enantiomers are crystalline and melt into a $S_A$ phase at 106°C, followed by a first order transition to an isotropic phase at 120°C. All monomer mixtures (S)-11/(R)-11(X/Y=90/10-10/90) are also crystalline and exhibit a $S_A$ phase. Additional crystalline phases are generated upon mixing these two enantiomers. As observed from Figure 7b, c and d, both enantiomers and their mixtures exhibit enantiotropic $S_A$, $S_C^*$ and $S_X$ phases in addition to the polymorphic crystalline phases. If we examine the DSC cooling scan from Figure 7d, we observe that there is no crystallization peak. however, there is an additional unidentified S phase in (S)-11/(R)-11(X/Y) with X/Y=3/7-7/3. The nature of these $S_X$, $S_{X'}$ and crystalline phases is not yet clear at present time and is not of main concern for this paper. The dependence of all phase transition temperatures on enantiomeric composition (or enantiomeric excess) is illustrated in Figure 8. The highest crystalline melting temperature decreased as the enantiomeric excess of the mixtures decreases during the first heating scan (Figure 8a), while in Figure 8b and c, these two enantiomers are miscible and therefore isomorphic in the $S_A$, $S_C^*$ and $S_X$ phases over the entire range of enantiomeric composition.

In order to further confirm the $S_C^*$ and $S_A$ phases of both monomers and their mixtures. WAXS experiments were performed on both enantiomers and on their racemic mixture. The dependence of the layer spacing on temperature is shown in Figure 9a and b as obtained during the heating and cooling scans, respectively. In Figure 9a the layer spacings of both monomers do not change much with the increase in temperature in the crystalline phase until about 75°C when the

$S_C^*$ phase is formed. In the $S_C^*$ phase the layer spacing increases with the increase in temperature until it reaches a constant value (30.3 ± 0.5Å) at about 89°C when the $S_A$ phase is formed. Within the experimental error the experimental d-spacing of 30.3 ± 0.5Å is very close to the calculated value of the extended monomeric unit which is 32.6Å. Since the $S_C^*$-$S_A$ transition is covered by a crystalline phase in the racemic mixture, a sudden jump in d-spacing to 29.9Å was observed (Figure 9a). Data obtained during the cooling scan (Figure 9b) show a constant d-spacing in the $S_A$ phase, followed by a gradual decrease of the d-spacing in the $S_C^*$ phase during the cooling process. These results are in good agreement with the results obtained by DSC and optical polarized microscopy, and therefore, confirm the $S_C^*$ and $S_A$ phases of both monomers and of their mixtures.

The most significant observation in the mixtures of the two enantiomeric monomers is the upward curvature of the phase transition temperature from the $S_A$ phase to the isotropic phase (Figure 8) with a deviation of up to 2.4°C in the racemic mixture compared with that of the pure enantiomers. This indicates a very strong heterochiral molecular recognition in the $S_A$ phase of the enantiomeric mixture of (S)-11 and (R)-11 compared with other systems[1-4]. Based on the previous discussion a linear dependence is expected for the $S_A$-I transition temperature of (S)-11/(R)-11(X/Y) if they form an ideal solution since their transition temperatures and the associated enthalpy changes are identical. Instead, the $S_A$-I transition temperature of the monomer mixture shows an upward curvature, resulting in a positive deviation from the ideal solution behavior. This is an ideal mixture at the molecular level over which a strong interaction between the two enantiomers (S)-11 and (R)-11 is overlapped. Therefore, a very strong heterochiral recognition is observed between the two enantiomers in their $S_A$ phase. It is also observed that the $S_A$-$S_C^*$ transition temperatures display a downward curvature with a deviation of up to -3.2°C for the racemic mixture. This means that the two enantiomers do not form an ideal solution in the $S_C^*$ phase prior to $S_C^*$-$S_A$ transition. Similar behaviors were found in many other systems.[1-4,5] The other interesting phenomena are the positives curvatures of the $S_X$-$S_C^*$ and $S_C^*$-K transitions (Figure 8b) with a deviation of up to 7°C and 10°C, respectively, in the racemic mixture. This

observation indicates that there is a strong heterochiral recognition in the $S_X$ phase and also in the $S_C^*$ phase of (S)-11/(R)-11(X/Y). However, the recognition event in the $S_C^*$ phase occurs only below the crystallization temperature.

In summary, both enantiomeric monomers and their mixtures exhibit enantiotropic $S_A$, $S_C^*$ and $S_X$ phases in addition to polymorphic crystalline phases. Both enantiomers are miscible in their $S_A$, $S_C^*$ and $S_X$ phases over the entire range of composition. The dependence of the phase transition temperatures of monomer mixtures on enantiomeric excess demonstrated a non ideal solution behavior in their $S_A$, $S_C^*$ and $S_X$ phases and a strong heterochiral interaction in all these phases. In the last two phases this interaction occurs only below the crystallization temperature. The presence of such a strong chiral recognition is probably related to the unique structure of cyanohydrin ester group in the two enantiomeric monomers. The rigid -CN polar group in cyanohydrin ester was directly attached to the chiral center, and this chiral center was connected to the -COO- group directly. Such a structural feature could prevent the free rotation of the terminal chiral group, therefore maintaining a large dipole moment in the smectic layer. This could be the reason why the positive deviation is high (up to 2.4°C in $S_A$ phase) compared with similar data observed for other enantiomeric mixtures.[1,4,5] What makes it more interesting is that it represent the first example in which the chiral recognition is expended to the $S_C^*$ and $S_X$ phases in (S)-11/(R)-11(X/Y). A previous publication from our group has reported the first example in which chiral recognition was observed in the $S_C^*$ phase only in the mixtures of enantiomeric polymers based on (R)- and (S)-2-fluoro-4-methylpentyl 4'-(8-vinyloxyoctyloxy)biphenyl-4-carboxylate, but not in monomer mixtures.[5c]

## 4b) Mixtures of monomer with polymer

The DSC traces of the first and second heating, and the first cooling scans of the mixtures of (S)-11 with poly[(R)-11] with DP=4.4 are illustrated in Figure 10a, b and c, respectively. The corresponding phase diagrams are presented in Figure 11a, b, and c. The thermal transition temperatures and corresponding enthalpy changes are summarized in Table IV.

The first DSC scans (Figure 10a) show a decreased amount of crystallinity upon the mixing of (S)-11 with poly[(R)-11]. In the second heating scan (Figure 10b) the kinetically controlled crystalline phase is totally suppressed. As observed from the Figure 11b and c, the structural units of (S)-11 and poly[(R)-11] are miscible and isomorphic only in the $S_A$ and $S_C^*$ phases. $S_A$-I transition temperature seems to show a linear dependence over the entire composition range. Since the $\Delta H$ corresponding to $S_A$-I transition temperature for monomer (S)-11 is less than that of poly[(R)-11], the Schröder-van Laar equation predicts a positive curvature for an ideal solution. The net result is a nonideal behavior, and a negative deviation of up to -3.4°C from the theoretical values is observed. Therefore, there is no heterochiral recognition in the monomer/polymer mixtures. The $S_C^*$-$S_A$ transition temperature exhibits a downward curvature, and this also represents a nonideal solution behavior.

### 4c) Mixtures of polymers

Two sets of binary mixtures of poly[(S)-11] with poly[(R)-11] were prepared. Polymer mixture I consists of poly[(S)-11] with DP=4.6 and poly[(R)-11] with DP=4.4. Their molecular weights. $S_A$-I transition temperatures and corresponding enthalpy changes are close to each other. Polymer mixture II consists of poly[(S)-11] with DP=4.3 and poly[(R)-11] with DP=5.7. The molecular weight. $S_A$-I transition temperature and corresponding $\Delta H$ of poly[(R)-11] are higher than those of poly[(S)-11]. The characterization results are summarized in Tables 5 and 6. Figures 12 and 13 represent their first heating DSC traces and the corresponding phase diagrams, respectively. As we can see from Figure 12, the crystalline phase was suppressed upon mixing in both polymer mixtures. All mixtures are amorphous and exhibit enantiotropic $S_C^*$ and $S_A$ phases. The phase diagrams from Figure 13 indicate that the structural units of both polymers are miscible and isomorphic in their $S_A$ and $S_C^*$ phases for both mixtures. The $S_A$-I transition temperatures show a slightly negative curvature for both mixtures. Based on the previous discussion, the $S_A$-I transition temperature should show a linear dependence for the polymer mixture I and a positive curvature for the polymer mixture II if ideal solid solutions were formed.

The net result is a negative deviation (up to -1.6°C) for both mixtures from the ideal behavior, indicating that no heterochiral recognition exists in the $S_A$ phase of the polymer mixtures. The $S_C^*$-$S_A$ transition temperature also shows a negative curvature with a deviation of up to about -8.1°C for both polymer mixtures. This trend is similar to that of the present monomer/monomer mixtures and monomer/polymer mixtures, and that of other system.[3,5]

However, it is interesting that the glass transition temperature shows a positive curvature. Similar positive deviations of the glass transition temperature is well established for miscible polymer blends with strong interchain interactions.[21,22] This is probably due to strong intermolecular interactions between the enantiomeric structural units which leads to less free volume in the glassy state of the $S_C^*$ phase. Therefore, this result demonstrates a chiral molecular recognition effect in the $S_C^*$ which exists only below the glass transition temperature.

## 5. Summary

Based on the previous discussion, heterochiral molecular recognition was observed in pairs of enantiomeric monomers (S)-11/(R)-11(X/Y) in their $S_A$ phase and in their $S_C^*$ phase below crystallization and in $S_X$ phases. The recognition effect in the $S_X$ phase represents the second example of chiral molecular recognition observed in a tilted $S_C^*$ phase of enantiomeric pairs of low molar mass liquid crystals.[5c] The presence of a much stronger chiral recognition effect compared with previous systems[1-4,5] is probably due to the larger dipole present in the stereocenter of 11 which is directly coupled to the mesogen.

The chiral molecular recognition event observed in the $S_A$ phase of the monomer mixtures canceled in the corresponding mixtures involving polymers (monomer/polymer and polymer/polymer mixtures). Figure 14 illustrates the deviation of the isotropization temperature of various mixtures obtained as a function of the composition of R enantiomer. These deviations were calculated by the difference between the experimental and calculated values for an ideal solution using the Schröder-van Laar equation. As observed from Figure 14, only the $S_A$-I transition temperatures from monomer/monomer mixtures show a positive deviation of up to 2.4°C.

indicating the existence of heterochiral recognition in monomer mixtures. Each time when a polymer was involved in the mixture, a negative deviation of the $S_A$-I transition temperatures was observed. The chiral molecular recognition effects in the $S_C^*$ phase of monomers below crystallization and in polymers below glass transitions are of extreme fundamental interest. Scheme 3 outlines a possible mechanism for the heterochiral interaction between the stereocenters of (S)-11 and (R)-11 in an untilted layer phase like $S_A$. As illustrated in this scheme, heterochiral interaction can be envisioned to take place between the acidic hydrogen and the cyano groups of the two stereocenters when they are arranged in a layer structure like that encountered in a $S_A$ phase. Additional structural and modeling investigations are necessary to elucidate this possibility.

As demonstrated by the results of this and previous publications[1-5], layered liquid crystalline phases are providing an interesting alternative approach to quantitative studies on chiral molecular recognition which so far was investigated mostly with monolayers of enantiomers[23] and diastereomers.[24]


## ACKNOWLEDGMENTS

## REFERENCES

(1)   (a) Goodby, J. W.; Waugh, M. A.; Stein, S. M.; Chin, E.; Pindak, R.; Patel, J. S. *J. Am. Chem. Soc.* **1989**, *111*, 8119. (b) Slaney, A. J.; Goodby, J. W. *Liq. Cryst.* **1991**, *9*, 849. (c) Goodby, J. W.; Nishiyama, I.; Slaney, A. J.; Booth, C. J.; Toyne, K. J. *Liq. Cryst.* **1993**, *14*, 37. (d) Goodby, J. W.; Chin, E. *Liq. Cryst.* **1988**, *3*, 1245. (e) Goodby, J. W.; Patel, J. S.; Chin, E. *J. Mater. Chem.* **1992**, *2*, 197.

(2)   (a) Levelut, A. M.; Germain, C.; Keller, P.; Liebert, L.; Billard, J. *J. Phys., Paris* **1983**, *44*, 623. (b) Keller, P. *Mol. Cryst. Liq. Cryst. Lett.* **1984**, *102*, 295. (c) Billard, J.; Dahlgren, A.; Flatischler, K.; Lagerwall, S. T.; Otterholm, B. *J. Phys., Paris* **1985**, *46*, 1241. (d) Heppke, G.; Kleineberg, P.; Lötzsch, D. *Liq. Cryst.* **1993**, *14*, 67. (e) Nguyen, H. T.; Twieg, R. J.; Nabor, M. F.; Isaert, N.; Destrade, C. *Ferroelectrics* **1991**, *121*, 187. (f) Heppke, G.; Lötzsch, D.; Demus, D.; Diele, S.; Jahn, K.; Zaschke, H. *Mol. Cryst. Liq. Cryst.* **1991**, *208*, 9.

(3)   (a) Leclercq, M.; Billard, J.; Jacques, J. *Mol. Cryst. Liq. Cryst.* **1969**, *8*, 367. (b) Bahr, CH.; Heppke, G.; Sabaschus, B. *Ferroelectrics* **1988**, *84*, 103. (c) Bahr, CH.; Heppke, G.; Sabaschus, B. *Liq. Cryst.* **1991**, *9*, 31.

(4)   (a) Yamada, Y.; Mori, K.; Yamamoto, N.; Hayashi, H.; Nakamura, K.; (b) Yamawaki, M.; Orihara, H.; Ishibashi, Y. *Jpn. J. Appl. Phys.* **1989**, *28*, L1606. (c) Takezoe, H.; Lee, J.; Chandani, A. D. L.; Gorecka, E.; Ouchi, Y.; Fukuda, A.; Terashima, K.; Furukawa, K. *Ferroelectrics* **1991**, *114*, 187. (d) Takezoe, H.; Fukuda, A.; Ikeda, A.; Takanishi, Y.; Umemoto, T.; Watanabe, J.; Iwane, H.; Hara, M.; Itoh, K. *Ferroelectrics* **1991**, *122*, 167.

(5)   Percec, V.; Oda, H.; Rinaldi, P. L.; Hensley, D. R. *Macromolecules* **1994**, *27*, 12. (b) Percec, V.; Oda, H. *Macromolecules* submitted. (c) Percec, V.; Oda, H. *Macromolecules* submitted.

(6)   Percec, V. Tomazos, D. *Adv. Mater.* **1992**, *4*, 548.

7) (a) Percec, V.; Zheng, Q. *J. Mater. Chem.* **1992,** 2, 475. **(b)** Percec, V.; Zheng, Q.; Lee, M. *J. Mater. Chem.* **1991,** *1,* 611. (c) Percec, V.; Zheng, Q.; Lee, M. *J. Mater. Chem.* **1991,** *1,* 1015.

(8) Chan, L. K.; Gray, G. W.; Lacey, D.; Scrowston, R. M.; Shenouda, I. G.; Toyne, K. J. *Mol. Cryst. Liq. Cryst.* **1989,** *172,* 125.

(9) Chin, E.; Goodby, J. W. *Mol. Cryst. Liq. Cryst.* **1986,** *141,* 310.

(10) Moore, J. S.; Stupp, S. T. *Macromolecules* **1990,** 23, 65.

(11) Mitsunobu, O. *Synthesis* **1981,** 1.

(12) Botteghi,C., Chelucci G.; Marchetti, M. *Synthetic Communications* **1982,** *12,* 25.

(13) Faustini, F.; Munari, S. D.; Panzeri, A.; Villa, V., Gandolfi, C. A. *Tetrahedron Letters* **1981,** 22, 4533.

(14) Fu, S. J.; Birnbaum, S. M.; Greenstein, J. P. *J. Am. Chen. Soc.* **1954,** 76, 6056.

(15) Shibaev, V. P.; Kozlovsky, M. V.; Beresnev, N. A.; Blinov, L. M. *Polym. Sci. USSR* **1987,** 29, 1616.

(16) Mitsunobu, O.; Eguchi, M. *Bull. Chem. Soc. Jpn.* **1971,** 44, 3427.

(17) Grynkiewicz, G.; Burzynsky, H. *Tetrahedron* **1976,** 32, 2109.

(18) (a) Percec, V.; Lee, M. *Macromolecules* **1991,** 24, 1017. **(b)** Percec, V.; Zheng, Q. *J. Mater Chem.* **1992,** 2, 1041.

(19) a) Cho, C. G.; Feit, B. A.; Webster, O. W. *Macromolecules* **1990,** 23, 1918. (b) Cho, C. G.; Feit, B. A.; Webster, O. W. *Macromolecules* **1992,** 25, 2081. (c) Lin, C. H.; Matyjaszewsky, K. *Polym. Prepr., Am. Chem. Soc. Div. Polym. Chem.* **1990,** *31,* 599.

(20) Van Hecke, G. R. *J. Phys. Chem.* **1979,** 83, 2344.

(21) (a) Rodriguez-Parada, J. M.; Percec, V. *Macromolecules* **1986,** *19,* 55. (b) Rodriguez-Parada, J. M.; Percec, V. *J. Polym Sci. Polym. Chem. Ed.* **1986,** 24, 579. (c) Pugh, C; Rodriguez-Parada, J. M.; Percec, V. *J. Polym Sci. Polym. Chem. Ed.* **1986,** 24, 747. (d) Percec, V.; Schild, H. G.; Rodriguez-Parada, J. M.; Pugh, C. *J. Polym Sci. Polym. Chem. Ed.* **1988,** 26, 935.

(22) (a) Smith, K. L.; Winslow, A. E.; Perterson, D. E. *Polym. Eng. Sci.* **1959**, *16*, 593. (b) Akiyama, S; Komatsu, J; Kaneto, R. *Polym. J.* **1975**, *7*, 172. (c) Ting, S. P.; Pearce, E. M.; Kwei, T. K. *J. Polym. Sci., Polym. Lett. Ed.* **1980**, *18*, 201.

(23) (a) Arnetts, E. M.; Harvey, N. G.; Rose, P. L. *Acc. Chem. Res.* **1989**, *22*, 131. (b) Rose, P. L.; Harvey, N. G.; Arnett, E. M. In *Advances in Physical Organic Chemistry Vol. 28*; Bethell, D., Ed.; Academic Press: New York, 1993; p 45. (c) Arnett, E. M.; Thompson, O. *J. Am. Chem. Soc.* **1981**, *103*, 968. (d) Harvey, N. G.; Rose, P. L.; Mirajovsky, D.; Arnett, E. M. *J. Am. Chem. Soc.* **1990**, *112*, 3547. (e) Arnett, E. M.; Gold, J. M. *J. Am. Chem. Soc.* **1982**, *104*, 636.

(24) (a) Harvey, N.; Rose, P.; Porter, N. A.; Huff, J.; Arnett, E. M. *J. Am. Chem. Soc.* **1988**, *110*, 4395. (b) Heath, J. G.; Arnett, E. M. *J. Am. Chem. Soc.* **1992**, *114*, 4500.

# SCHEME AND FIGURE CAPTIONS

Scheme 1. Synthesis of (S)-1-cyano-2-methylpropyl 4'-{[4-(8-vinyloxyoctyl-oxy)benzoyl]oxy}biphenyl-4-carboxylate [(S)-11] and (R)-1-cyano-2-methylpropyl 4'-{[4-(8-vinyloxyoctyloxy)benzoyl]oxy}biphenyl-4-carboxylate [(R)-11].

Scheme 2. Mechanism of esterification of (S)-3 with 5 in the presence of DEAD/PPh$_3$ with inversion of configuration.

Scheme 3. Possible mechanism for heterochiral interaction between the stereocenters of (S)-11 and (R)-11.

Figure 1. Representative $^1$H-NMR spectra of monomer (S)-11 ([(S)-11]=0.038M): (a) without shift reagent: (b) with shift reagent ([Eu(hfc)$_3$]=0.011M).

Figure 2. Representative $^1$H-NMR spectra of the binary mixture of monomers (S)-11/(R)-11(X/Y) with X/Y=2/1 ([(S)-11]=0.038M, [(R)-11]=0.019 M): (a) without shift reagent: (b) with shift reagent ([Eu(hfc)$_3$]=0.014M).

Figure 3. The dependence of number-average molecular weight (Mn) and polydispersity (Mw/Mn) of poly[(S)-11] (open symbols) and poly[(R)-11] (closed symbols) determined by GPC on the [M]$_0$/[I]$_0$ ratio.

Figure 4. DSC traces of polymers with different degrees of polymerization (DP) determined by GPC. DP is printed on the top of each DSC scan (heating rate: 20°C/min): (a) poly[(S)-11]: (b) poly[(R)-11].

Figure 5. The dependence of phase transition temperatures on DP of poly[(S)-11] (open symbols) and poly[(R)-11] (closed symbols): ●, ○: T(g-S$_C$*, S$_X$); ■, □: T(S$_X$-S$_C$*); ◆, ◇: T(k-S$_C$*); ■, □: T(S$_C$*-S$_A$); ▲, △: T(S$_A$-i).

Figure 6. (a) Representative wide angle X-ray scattering patterns of poly[(S)-11] with DP=19.7 in S$_X$, S$_A$ and S$_C$* phases; (b) The dependence of the layer spacings of poly[(S)-11] with DP=17.3 and poly[(R)-11] with DP = 19.7 on temperature determined by wide angle X-ray scattering experiments during the heating scan (2.5°C/min).

Figure 7.  DSC traces of (S)-11 and (R)-11 and their binary mixtures. The composition of the binary mixtures is printed on the top of each DSC scan (10°C/min): (a) first heating scan; (b) second heating scan; (c) heating scan after cooling to 50°C; (d) first cooling scan.

Figure 8.  The dependence of the phase transition temperatures on the composition of binary mixtures of (S)-11 and (R)-11. (a) first heating scan: ❑: $T(S_A\text{-}i)$; ▲: $T(k\text{-}S_A)$; ■, ●: $T(k\text{-}k)$; ◢: $T(k\text{-}k)$, crystallization; (b) combination of second heating scan and heating scan after cooling to 50°C: ❑: $T(S_A\text{-}i)$; Δ: $T(S_C^*\text{-}S_A)$; ■: $T(k\text{-}S_C^*)$; ▲, ▼, ●: $T(k\text{-}k)$; ◧, ◩, ◪ : $T(k\text{-}k)$, crystallization; ◢: $T(S_C^*\text{-}k)$, crystallization; ◨: $T(S_X\text{-}S_C^*)$; (c) first cooling scans: ❑: $T(i\text{-}S_A)$; Δ: $T(S_A\text{-}S_C^*)$; ◨: $T(S_C^*\text{-}S_X)$; ⊕: $T(S_X\text{-}S_{X'})$.

Figure 9.  The dependence of the layer spacings of (S)-11, (R)-11 and their racemic mixture on temperature determined by wide angle X-ray scattering experiments (2.5°C/min): (a) during heating scan; (b) during cooling scan.

Figure 10.  DSC traces of the binary mixtures of (S)-11 and poly[(R)-11] with DP=4.4. The composition of the binary mixtures is printed on the top of each DSC scan (10°C/min). (a) first heating scan; (b) second heating scan; (c) first cooling scan.

Figure 11.  The dependence of phase transition temperatures on composition of binary mixtures of (S)-11 and poly[(R)-11] with DP=4.4: (a) first heating scan: ❑: $T(S_A\text{-}i)$; Δ: $T(S_C^*\text{-}S_A)$; ▲: $T(k\text{-}S_C^*, S_A)$; ■: $T(k\text{-}k)$; ○: $T(g\text{-}k)$; (b) second heating scan: ❑: $T(S_A\text{-}i)$, Δ: $T(S_C^*\text{-}S_A)$; ■: $T(k\text{-}k)$; ◻: $T(k\text{-}k)$, crystallization; ◐: $T(S_C^*\text{-}k)$, crystallization; ⊕: $T(S_X\text{-}S_C^*)$; ○: $T(g\text{-}S_C^*)$; (c) first cooling scan: ❑: $T(i\text{-}S_A)$; Δ: $T(S_A\text{-}S_C^*)$; ◨: $T(S\text{-}S_X)$; ○: $T(S_C^*\text{-}g)$.

Figure 12.  DSC traces of the binary mixtures of poly[(S)-11] and poly[(R)-11]. The composition of the binary mixtures is printed on the top of each DSC scan (10°C/min, first heating scan): (a) binary mixtures of poly[(S)-11] with DP=4.6 and poly[(R)-11] with DP=4.4; (b) binary mixtures of poly[(S)-11] with DP=4.3 and poly[(R)-11] with DP=5.7.

Figure 13. The dependence of phase transition temperatures on the composition of binary mixtures of poly[(S)-11] and poly[(R)-11]. (a) first heating scan of binary mixture of poly[(S)-11] with DP=4.6 and poly[(R)-11] with DP=4.4; (b) first heating scan of binary mixtures of poly[(S)-11] with DP=4.3 and poly[(R)-11] with DP=5.7. $\Box$: $T(S_A$-i); $\Delta$: $T(S_C^*$-$S_A$); $\bigcirc$: $T(g$-$S_C^*, k)$; $\blacksquare$: $T(k$-$S_C^*)$.

Figure 14. The dependence of the deviation of $S_A$-I transition temperatures of various mixtures on the composition of (R)-enantiomer calculated by the difference between the experimental values obtained during the first heating scan and the calculated values for ideal solution using the Schröder-van Laar equation:
$\Box$: (S)-11/(R)-11;
$\blacksquare$: 11S/poly[(R)-11] with DP=4.4;
$\blacksquare$: poly[(S)-11] with DP=4.6/poly[(R)-11] with DP=4.4;
$\blacktriangle$: poly[(S)-11] with DP=4.3/poly[(R)-11] with DP=5.7.

Table 1. Cationic polymerization of (S)-11 (temperature: 0°C; solvent: $CH_2Cl_2$; $[M]_o=0.2$; $[(CH_3)_2SI_o/II_o = 10$; time: 1h) and characterization of the resulting poly[(S)-11].

| Sample No. | $[M]_o/I_{Io}$ | Polymer yield (%) | $Mn \times 10^{-3}$ | Mw/Mn | DP | Thermal transition temperatures[a] (°C) and corresponding enthalpy changes (kcal/mru) |
|---|---|---|---|---|---|---|
| 1 | 2 | 49 | 2.59 | 1.13 | 4.6 | g 8.5 k 54.4 (0.05) $S_{C^*}$ 117.0 (0.06) $S_A$ 173.1 (1.30) i |
| 2 | 3 | 54 | 3.05 | 1.16 | 5.4 | g 17.0 k 54.0 (0.28) $S_{C^*}$ 124.0 (0.03) $S_A$ 189.0(1.49) i |
| 3 | 5 | 59 | 3.74 | 1.18 | 6.6 | g 21.0 $S_{C^*}$ 130.7 (0.09) $S_A$ 195.3 (1.35) i |
| 4 | 8 | 65 | 5.79 | 1.11 | 10.2 | g 33.2 $S_x$ 64.8 (0.02) $S_{C^*}$ 142.8 (0.06) $S_A$ 226.8 (1.44) i |
| 5 | 12 | 69 | 7.17 | 1.13 | 12.6 | g 37.8 $S_x$ 82.1 (0.03) $S_{C^*}$ 144.7 (0.03) $S_A$ 242.8 (1.39) i |
| 6 | 18 | 53 | 9.71 | 1.10 | 17.0 | g 38.0 $S_x$ 93.4 (0.04) $S_{C^*}$ 149.0 (0.04) $S_A$ 247.0 (1.57) i |
| 7 | 25 | 62 | 11.2 | 1.12 | 19.7 | g 40.0 $S_x$ 108.0 (0.03) $S_{C^*}$ 151.6 (0.06) $S_A$ 251.8 (1.41) i |
| 8 | 30 | 70 | 11.7 | 1.12 | 20.6 | g 40.0 $S_x$ 109.8 (0.08) $S_{C^*}$ 152.4 (0.05) $S_A$ 253.0 (1.36) i |

a: Only first heating data (at heating rate = 20 °C/min) are reported. Subsequent heating and cooling were performed and it was found that samples with DP ≥ 6 decomposed. ^{1}H-NMR spectra from the decomposed samples suggested that the cyanohydrin ester linkage was cleaved above 200°C.

Table 2. Cationic polymerization of **(R)-11** (temperature: 0°C; solvent: $CH_2Cl_2$; $[M]_0=0.2$; $[(CH_3)_2S]_0/[I]_0=10$; time: 1h) and characterization of the resulting poly[**(R)-11**].

| Sample No. | $[M]_0/[I]_0$ | Polymer yield (%) | $Mn \times 10^{-3}$ | Mw/Mn | DP | Thermal transition temperatures[a] (°C) and corresponding enthalpy change (kcal/mru) |
|---|---|---|---|---|---|---|
| 1 | 2 | 51 | 2.43 | 1.16 | 4.4 | g 8.0 k 55.2 (0.05) $S_C^*$ 116.8 (0.06) $S_A$ 171.9 (1.26) i |
| 2 | 3 | 53 | 3.22 | 1.10 | 5.7 | g 20.0 k 54.1 (0.10) $S_C^*$ 123.6 (0.03) $S_A$ 189.0(1.46) i |
| 3 | 5 | 62 | 4.32 | 1.15 | 7.6 | g 24.5 $S_C^*$ 135.4 (0.10) $S_A$ 199.3 (1.54) i |
| 4 | 8 | 66 | 6.25 | 1.11 | 10.9 | g 32.4 $S_X$ 67.9 (0.02) $S_C^*$ 138.8 (0.06) $S_A$ 221.1 (1.24) i |
| 5 | 12 | 65 | 7.54 | 1.15 | 13.2 | g 38.1 $S_X$ 77.4 (0.03) $S_C^*$ 144.2 (0.04) $S_A$ 244.3 (1.51) i |
| 6 | 18 | 70 | 8.95 | 1.12 | 15.7 | g 39.0 $S_X$ 96.3 (0.05) $S_C^*$ 146.0 (0.05) $S_A$ 244.4 (1.42) i |
| 7 | 25 | 68 | 9.88 | 1.09 | 17.3 | g 40.0 $S_X$ 106.3 (0.03) $S_C^*$ 151.0(0.07) $S_A$ 247.4 (1.34) i |
| 8 | 30 | 68 | 11.2 | 1.20 | 19.7 | g 40.0 $S_X$ 107.0 (0.09) $S_C^*$ 149.7(0.03) $S_A$ 252.2 (1.38) i |

a: Only first heating data (at heating rate = 20 °C/min) are reported. Subsequent heating and cooling were performed and it was found that samples with DP ≥ 6 decomposed. $^1$H-NMR spectra from the decomposed samples suggested that the cyanohydrin ester linkage was cleaved above 200°C.

Table 3. Characterization of enantiomeric binary mixture of (S)-11 and (R)-11.

| Sample Number | Molar Ratio (S)-11/(R)-11 | Phase transition temperature(°C) and corresponding enthalpy changes(kcal/mru)[a] — Heating[b] | Cooling |
|---|---|---|---|
| 1 | 100/0 | k 106.2 (11.3) S$_A$ 120.1 (0.77) i — S$_X$ 0.3 (0.14) S$_C$* 12.7 (-2.05) k 39.6 (-2.36) k 69.7 (5.28) k 77.3 (3.02) S$_C$* 89.4 (0.10) S$_A$ 120.2 (0.80) i | i 116.7 (0.77) S$_A$ 86.4 (0.09) S$_C$* -2.31 (0.31) S$_X$ |
| 2 | 90/10 | k 58.9 (-0.20) k 88.2 (+*) k 103.2 (10.31) S$_A$ 120.1 (0.82) i — S$_X$ 2.3 (0.22) S$_C$* 16.2 (-2.44) k 45.7 (-2.63) k 70.2 (7.6) S$_C$* 89.2 (0.09) S$_A$ 121.2 (0.78) i | i 117.9 (-0.76) S$_A$ 85.7 (-0.09) S$_C$* -1.67 (0.23) S$_X$ |
| 3 | 80/20 | k 64.5 (3.71) k 67.2 (-4.70) k 89.0 (+*) k 100.3 (9.47) S$_A$ 121.6 (0.77) i — S$_X$ 2.6 (0.31) S$_C$* 17.23 (-2.53) k 55.8 (1.82) k 58.1 (-2.83) k 65.7 (+*) k 70.2 (6.34) k 79.3 (0.09) S$_C$* 87.9 (0.07) S$_A$ 121.6 (0.78) i | i 118.0 (-0.72) S$_A$ 84.5 (-0.08) S$_C$* -1.75 (-0.42) S$_X$ |
| 4 | 70/30 | k 63.2 (3.59) k 65.8 (-2.09) k 84.3 (+*) k 88.0 (+*) k 95.5 (9.77) S$_A$ 121.7 (0.75) i — S$_X$ 3.28 (0.41) S$_C$* 18.03 (-2.71) k 56.4 (4.36) k 59.3 (-*) k 65.6 (+*) k 67.2 (-2.13) k 82.4 (4.29) [S$_C$* 87.0 (0.05)]$^c$ S$_A$ 121.9 (0.77) i | i 118.5 (0.74) S$_A$ 83.9 (-0.08) S$_C$* -1.26 (-*) S$_X$ -7.52 (-0.34) |
| 5 | 60/40 | k 62.9 (1.62) k 66.6 (-0.67) k 84.8 (7.89) k 93.3 (0.27) S$_A$ 122.4 (0.76) i — S$_X$ 6.98 (0.66) S$_C$* 21.71 (-2.82) k 49.7 (-*) k 55.3 (+*) k 57.9 (-1.51) k 84.9 (8.15) [S$_C$* 86.8 (0.05)]$^c$ S$_A$ 122.6 (0.77) i | i 118.9 (-0.76) S$_A$ 83.4 (-0.08) S$_C$* -1.10 (-*) S$_X$ -5.63 (-0.44) |
| 6 | 50/50 | k 63.6 (0.99) k 67.9 (-0.31) k 86.4 (9.01) S$_A$ 122.4 (0.77) i — S$_X$ 7.36 (0.73) S$_C$* 22.50 (-2.86) k 46.5 (-1.61) k 72.2 (-0.55) k 85.9 (8.88) [S$_C$* 86.3 (0.05)]$^c$ S$_A$ 122.5 (0.74) i | i 118.8 (-0.74) S$_A$ 83.2 (-0.07) S$_C$* -1.18 (-*) S$_X$ -5.05 (-0.46) S$_X$' |
| 7 | 40/60 | k 62.2 (1.50) k 66.1 (-0.28) k 84.5 (8.12) k 93.4 (0.27) S$_A$ 121.8 (0.80) i — S$_X$ 6.77 (0.69) S$_C$* 20.97 (-2.80) k 48.0 (-*) k 55.0 (+*) k 57.4 (-1.61) k 84.4 (8.48) [S$_C$*86.2 (0.05)]$^c$ i | i 118.5 (-0.76) S$_A$ 83.3 (-0.07) S$_C$* -1.26 (-*) S$_X$ -5.75 (-0.40) S$_X$' |
| 8 | 30/70 | k 63.7 (2.43) k 66.4 (-2.72) k 84.8 (+*) k 88.7 (+*) k 95.6 (9.76) S$_A$ 121.6 (0.78) i — S$_X$ 3.98 (0.65) S$_C$* 17.80 (-2.71) k 56.8 (3.01) k 59.2 (-*) k 65.8 (+*) k 67.5 (-2.15) k 82.9 (5.6) [S$_C$* 86.9 (0.09)]$^c$ S$_A$ 121.7 (0.79) i | i 118.2 (-0.76) S$_A$ 83.6 (-0.09) S$_C$* -1.65 (-*) S$_X$ -7.56 (-0.40) S$_X$' |
| 9 | 20/80 | k 64.3 (3.83) k 67.2 (-4.01) k 88.9 (+*) k 100.0 (12.7) S$_A$ 121.3 (0.81) i — S$_X$ 2.1 (0.31) S$_C$* 16.4 (-2.56) k 55.6 (1.90) k 57.7 (-3.10) k 65.5 (+*) k 70.0 (6.37) k 79.3 (0.1) S$_C$* 7.4 (0.08) S$_A$ 121.3 (0.79) i | i 117.7 (-0.76) S$_A$ 84.1 (-0.08) S$_C$* -2.35 (-0.32) S$_X$ |
| 10 | 10/90 | k 57.8 (-0.11) k 88.2 (+*) k 103.1 (11.04) S$_A$ 121.0 (0.82) i — S$_X$ 1.5 (0.20) S$_C$* 14.90 (-2.47) k 46.2 (-2.36) k 70.6 (8.2) S$_C$* 88.9 (0.09) S$_A$ 121.1 (0.83) i | i 117.5 (-0.80) S$_A$ 85.5 (-0.09) S$_C$* -2.34 (-0.41) S$_X$ |
| 11 | 0/100 | k 106.1 (11.0) S$_A$ 120.0 (0.77) i — S$_X$ 0.2 (0.13) S$_C$* 12.2 (-1.80) k 38.7 (-2.08) k 69.7 (4.91) k 77.7 (3.39) S$_C$* 89.7 (0.10) S$_A$ 120.0 (0.78) i | i 116.4 (-0.75) S$_A$ 86.3 (-0.10) S$_C$* -2.22 (-0.30) S$_X$ |

a: DSC scan rate = 10°C/min; b: Data on the first line are collected from first heating scan. Data on the second and third line are collected from second heating scan. c: Monotropic mesophase, data are collected from the third heating scan. *: Overlap peak, +, - sign indicate endo and exo, respectively.

Table 4. Characterization of binary mixture of (S)-11 and poly[(R)-11] with DP=4.4. Data on the first and second line are from the first and second heating scans, respectively.
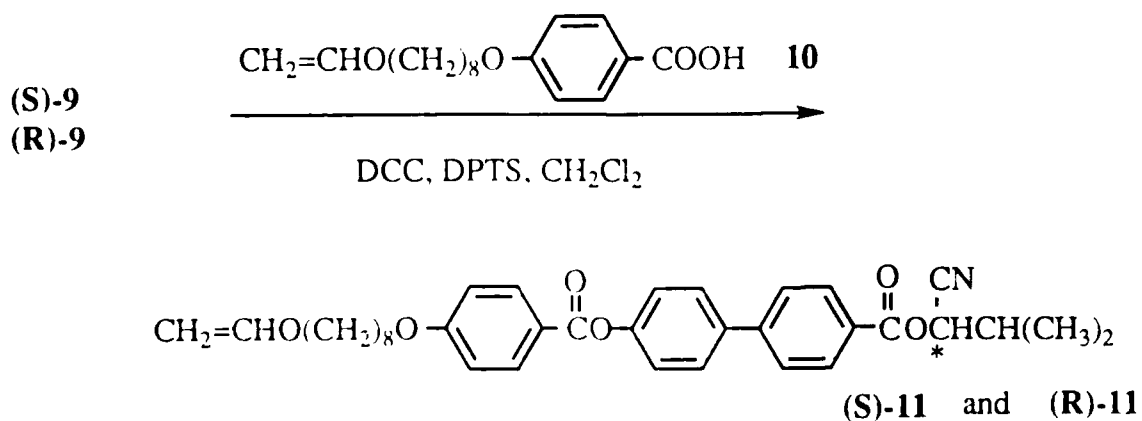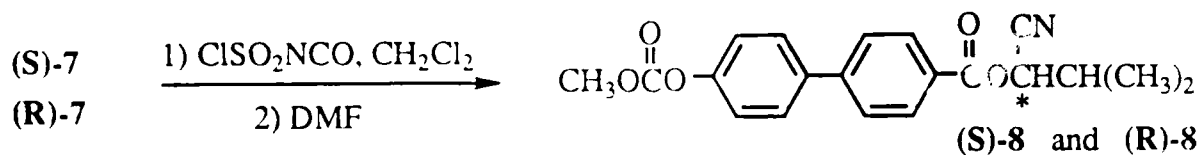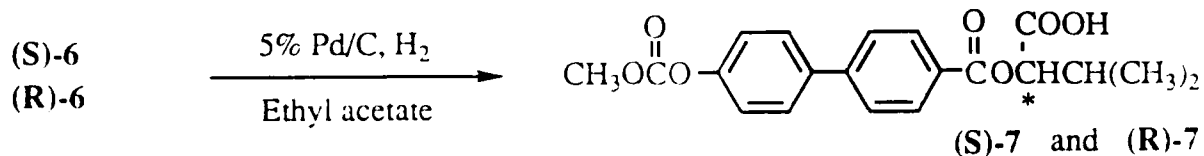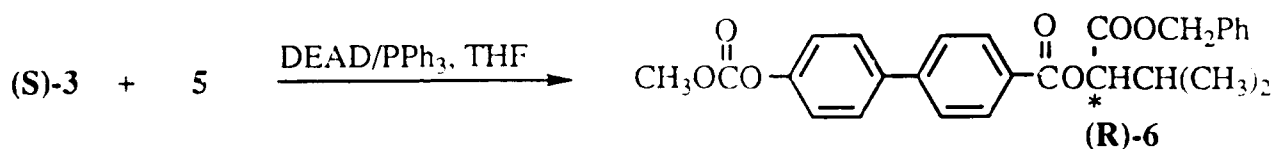
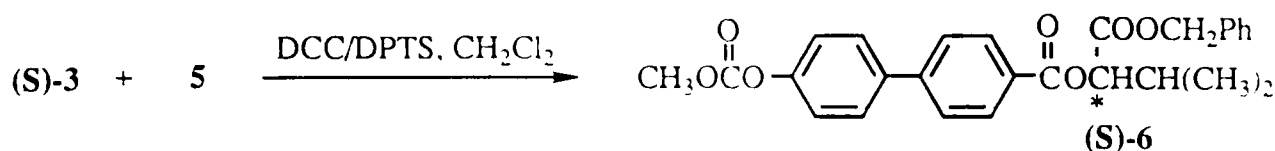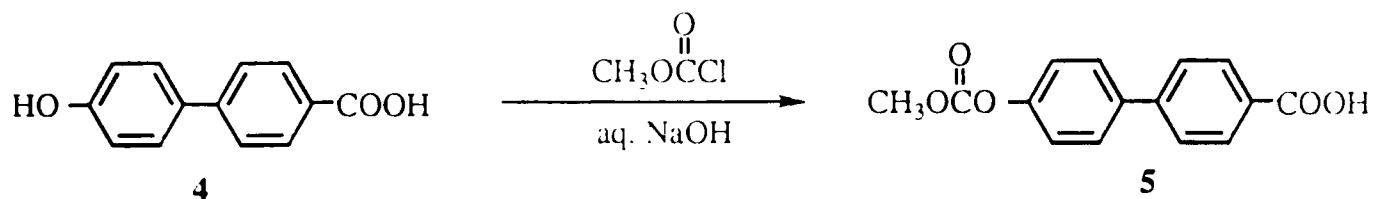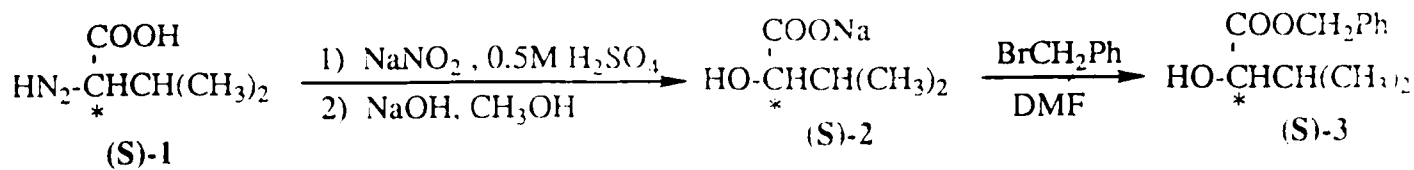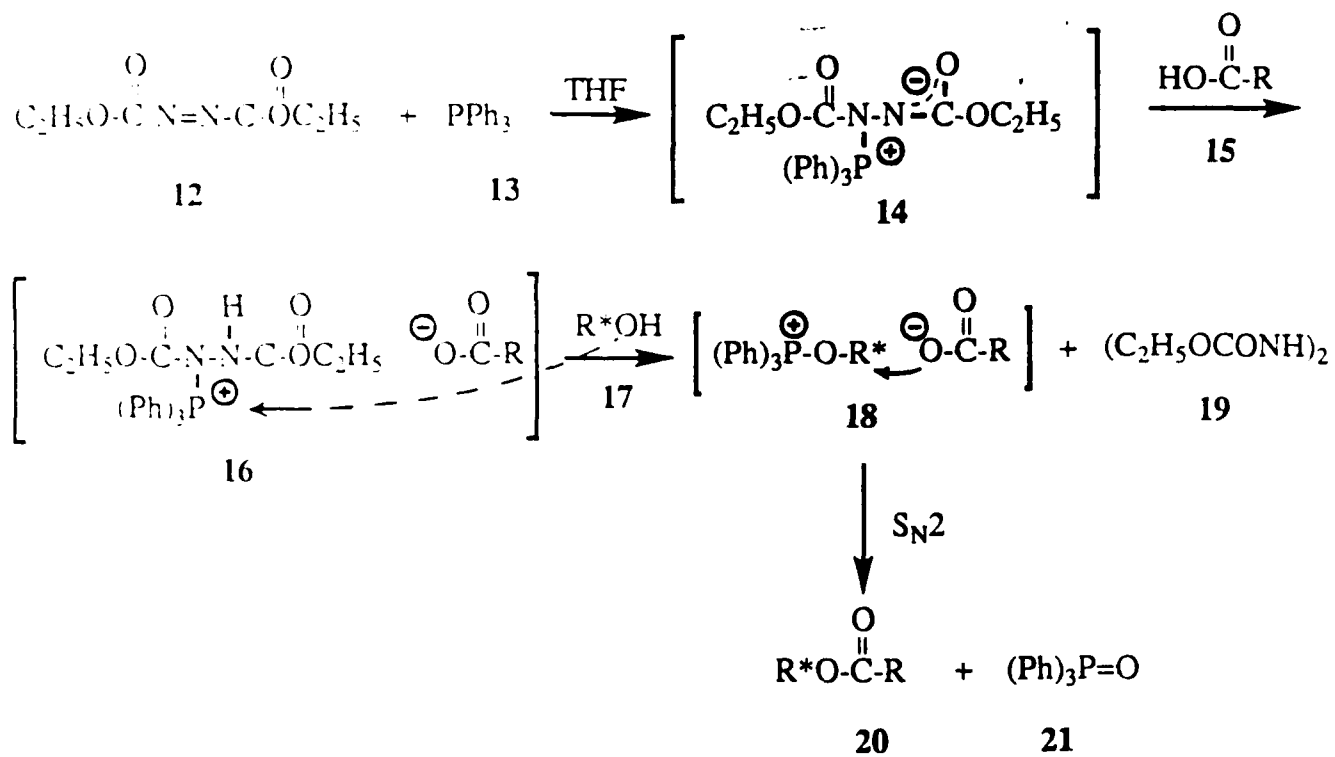| Sample | Polymer composition (S)-11/Poly[(R)-11] | Thermal transition temperatures (°C) and corresponding enthalpy change (kcal/mru) | |
|---|---|---|---|
| | | Heating | Cooling |
| 1 | 100/0 | k 106.2 (11.3) $S_A$ 120.1 (0.77) i<br>$S_X$ 0.3 (0.14) $S_C^*$ 12.7 (-2.05) k 39.6 (-2.36) k 69.7 (5.28)<br>k 77.3 (3.02) $S_C^*$ 89.4 (0.10) $S_A$ 120.2 (0.80) i | i 116.7 (-0.77) $S_A$ 86.4 (-0.09) $S_C^*$ -2.31 (-0.31) $S_X$ |
| 2 | 80/20 | k 62.6 (1.94) k 67.0 (-3.44) k 102.9 (7.38) $S_A$ 129.9 (0.86) i<br>$S_X$ -0.6 (0.20) $S_C^*$ 86.9 (0.06) $S_A$ 131.9 (0.86) i | i 127.8 (-0.82) $S_A$ 84.5 (-0.04) $S_C^*$ -4.9 (-0.30) $S_X$ |
| 3 | 65/35 | k 39.5 (0.32) k 98.1 (5.76) $S_A$ 139.0 (1.03) i<br>$S_X$ 1.4 (0.17) $S_C^*$ 85.6 (0.08) $S_A$ 139.7 (0.79) i | i 135.3 (-0.89) $S_A$ 82.4 (-0.03) $S_C^*$ -2.9 (-0.30) $S_X$ |
| 4 | 50/50 | k 43.5 (0.13) k 90.2 (0.71) $S_A$ 144.6 (1.07) i<br>g -4.9 $S_C^*$ 88.6 (0.05) $S_A$ 145.8 (1.03) i | i 141.7 (-0.86) $S_A$ 85.2 (-0.05) $S_C^*$ -7.2 g |
| 5 | 35/65 | g 2.7 k 85.3 (0.82) $S_A$ 155.9 (1.00) i<br>g -1.0 $S_C^*$ 84.7 (0.02) $S_A$ 154.3 (1.14) i | i 149.6 (-1.00) $S_A$ 81.7 (-0.02) $S_C^*$ -4.3 g |
| 6 | 20/80 | g 3.5 k 73.5 (0.20) $S_C^*$ 95.5 (0.04) $S_A$ 160.7 (1.06) i<br>g 2.5 $S_C^*$ 95.8 (0.06) $S_A$ 161.2 (1.03) i | i 156.8 (-1.11) $S_A$ 92.3 (-0.07) $S_C^*$ -2.9 g |
| 7 | 0/100 | g 4.5 k 52.6 (0.18) $S_C^*$ 115.6 (0.07) $S_A$ 170.8 (1.31) i<br>g 4.4 $S_C^*$ 113.0 (0.06) $S_A$ 170.3 (1.25) i | i 165.9 (-1.10) $S_A$ 110.7 (-0.06) $S_C^*$ -0.72 g |

Table 5. Characterization of enantiomeric binary mixture of poly[(S)-11] with DP=4.6 and poly[(R)-11] with DP=4.4. Data are collected from the first heating scan.
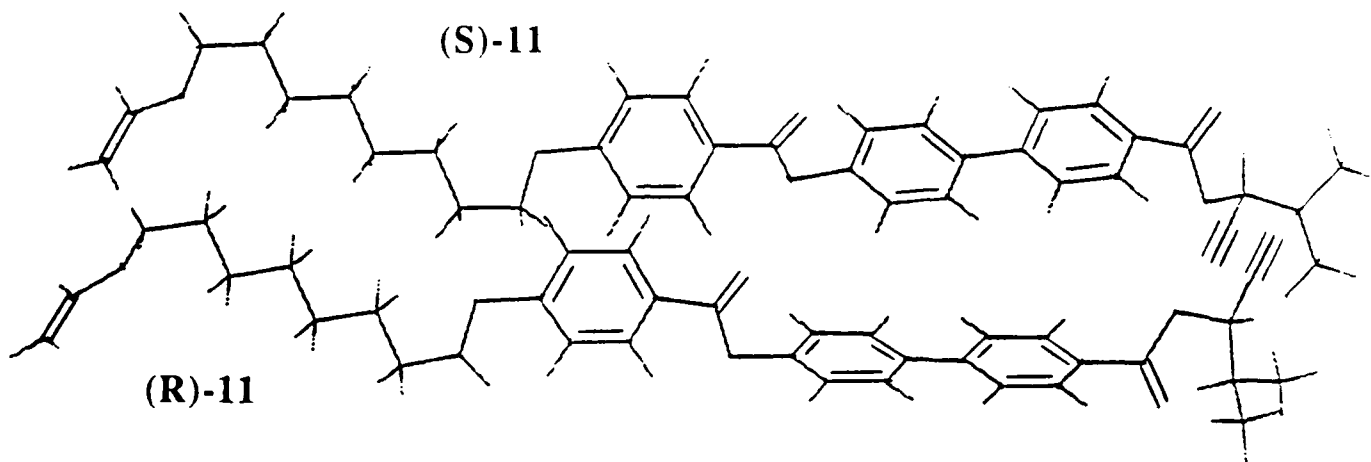
| Sample | Polymer composition Poly[(S)-11]/Poly[(R)-11] | Thermal transition temperatures (°C) and correspounding enthalpy change (kcal/mru) |
|---|---|---|
| 1 | 100/0 | g 5.2 k 49.7 (0.26) $S_C^*$ 115.8 (0.07) $S_A$ 171.8 (1.27) i |
| 2 | 80/20 | g 5.9 $S_C^*$ 108.7 (0.04) $S_A$ 171.2 (1.26) i |
| 3 | 65/35 | g 5.9 $S_C^*$ 108.0 (0.06) $S_A$ 171.2 (1.31) i |
| 4 | 50/50 | g 8.5 $S_C^*$ 107.5 (0.07) $S_A$ 170.2 (1.20) i |
| 5 | 35/65 | g 7.4 $S_C^*$ 107.8 (0.04) $S_A$ 171.0 (1.27) i |
| 6 | 20/80 | g 5.9 $S_C^*$ 110.2 (0.05) $S_A$ 170.9 (1.29) i |
| 7 | 0/100 | g 4.5 k 52.6 (0.18) $S_C^*$ 115.6 (0.07) $S_A$ 170.8 (1.31) i |

Table 6. Characterization of enantiomeric binary mixture of poly[(S)-11] with DP=4.3 and poly[(R)-11] with DP=5.7. Data are collected from the first heating scan.

| Sample | Polymer composition Poly[(S)-11]/Poly[(R)-11] | Thermal transition temperatures (°C) and correspounding enthalpy change (kcal/mru) |
| --- | --- | --- |
| 1 | 100/0 | g 3.1 k 45.6 (0.25) $S_C^*$ 112.1 (0.06) $S_A$ 167.5 (1.25) i |
| 2 | 80/20 | g 4.1 $S_C^*$ 107.3 (0.04) $S_A$ 169.9 (1.18) i |
| 3 | 65/35 | g 7.0 $S_C^*$ 106.6 (0.03) $S_A$ 172.1 (1.18) i |
| 4 | 50/50 | g 8.5 $S_C^*$ 106.7 (0.04) $S_A$ 174.1 (1.30) i |
| 5 | 35/65 | g 9.7 $S_C^*$ 108.3 (0.04) $S_A$ 176.4 (1.38) i |
| 6 | 20/80 | g 10.7 $S_C^*$ 111.9 (0.05) $S_A$ 178.8 (1.47) i |
| 7 | 0/100 | g 11.3 k 52.2 (0.50) $S_C^*$ 117.3 (0.04) $S_A$ 183.2 (1.37) i |

**(S)-1** → 1) $NaNO_2$, 0.5M $H_2SO_4$ 2) NaOH, $CH_3OH$ →

COOH / $HN_2$-CHCH$(CH_3)_2$ * **(S)-1**

COONa / HO-CHCH$(CH_3)_2$ * **(S)-2**

$BrCH_2Ph$ / DMF →

COOCH$_2$Ph / HO-CHCH$(CH_3)_2$ * **(S)-3**

HO—⬡—⬡—COOH **4**  →  $CH_3OCCl$ (O) / aq. NaOH  →  $CH_3OCO$—⬡—⬡—COOH **5**

**(S)-3** + **5** → DCC/DPTS, $CH_2Cl_2$ → **(S)-6**

**(S)-3** + **5** → DEAD/PPh$_3$, THF → **(R)-6**

**(S)-6** / **(R)-6** → 5% Pd/C, H$_2$ / Ethyl acetate → **(S)-7** and **(R)-7**

**(S)-7** / **(R)-7** → 1) $ClSO_2NCO$, $CH_2Cl_2$ 2) DMF → **(S)-8** and **(R)-8**

**(S)-8** / **(R)-8** → 30 % $NH_4OH$ in EtOH → **(S)-9** and **(R)-9**

**(S)-9** / **(R)-9** → $CH_2$=CHO$(CH_2)_8$O—⬡—COOH **10** / DCC, DPTS, $CH_2Cl_2$ →

$CH_2$=CHO$(CH_2)_8$O—⬡—CO—O—⬡—⬡—COCHCH$(CH_3)_2$ (CN) **(S)-11** and **(R)-11**

Scheme 1.

$$C_2H_5O\text{-}C(=O)\text{-}N=N\text{-}C(=O)\text{-}OC_2H_5 \quad + \quad PPh_3 \quad \xrightarrow{\text{THF}} \quad \left[ \begin{array}{c} \text{-}O \qquad \ominus O \\ C_2H_5O\text{-}C\text{-}N\text{-}N=C\text{-}OC_2H_5 \\ (Ph)_3P^{\oplus} \end{array} \right] \xrightarrow[\mathbf{15}]{HO\text{-}C(=O)\text{-}R}$$

**12**  ·  **13**  ·  **14**

$$\left[ \begin{array}{c} O \quad H \quad O \qquad \ominus O \\ C_2H_5O\text{-}C\text{-}N\text{-}N\text{-}C\text{-}OC_2H_5 \quad O\text{-}C\text{-}R \\ (Ph)_3P^{\oplus} \end{array} \right] \xrightarrow[\mathbf{17}]{R^*OH} \left[ (Ph)_3\overset{\oplus}{P}\text{-}O\text{-}R^* \quad \overset{\ominus}{O}\text{-}C(=O)\text{-}R \right] \quad + \quad (C_2H_5OCONH)_2$$

**16**  ·  **18**  ·  **19**

$$\downarrow S_N2$$

$$R^*O\text{-}C(=O)\text{-}R \quad + \quad (Ph)_3P=O$$

**20**  ·  **21**

Schem 2.

(S)-11

(R)-11

Scheme 3.

(a) (S)-11

(b) (S)-11 + Eu(hfc)₃

Figure 1.

(S)-11/(R)-11=2/1

(a)

5.48 (J=6.0)

h

δ (ppm)

(S)-11/(R)-11=2/1 + Eu(hfc)3

(b)

6.14 (J=6.0) from (R)-11    6.02 (J=6.0) from (S)-11

h

δ (ppm)

Figure 2.

Figure 3.

(a) Poly[(S)-11]

DP

4.6  K  S$_C^*$  S$_A$

5.4  K  S$_C^*$  S$_A$

6.6  S$_C^*$  S$_A$

10.1  S$_X$  S$_C^*$  S$_A$

12.6  S$_X$  S$_C^*$  S$_A$

17.0  S$_X$  S$_C^*$  S$_A$

19.7  S$_X$  S$_C^*$  S$_A$

20.6  S$_X$  S$_C^*$  S$_A$

ENDO ←

-10  50  110  170  230  290

(b) Poly[(R)-11]

DP

4.3  K  S$_C^*$  S$_A$

5.7  K  S$_C^*$  S$_A$

7.6  S$_C^*$  S$_A$

10.9  S$_X$  S$_C^*$  S$_A$

13.2  S$_X$  S$_C^*$  S$_A$

15.7  S$_X$  S$_C^*$  S$_A$

17.3  S$_X$  S$_C^*$  S$_A$

19.7  S$_X$  S$_C^*$  S$_A$

ENDO ←

-10  50  110  170  230  290

Figure 5.

Figure 6.

**(S)-11/(R)-11** (a)

**(S)-11/(R)-11** (b)

Figure 7

Figure 7.

Figure 9.

Figure 10.

Figure 12

Figure 13.

Figure 14.